Escola Tècnica Superior
d'Enginyeria Industrial de Barcelona
UNIVERSITAT POLITÈCNICA DE CATALUNYA

EFFECT OF THE LIGAND IN THE MODELING THE 3D STRUCTURE OF THE M3 MUSCARINIC RECEPTOR

BAHAREH RASAEIFAR

Supervised by

Juan Jesus Perez

A thesis submitted in partial fulfilment of a Master's degree in Biotechnological engineering

November 2013

Table of Contents

List of Figures

List of Tables

Abstract

There are still many question open to completely understand the structure-activity relationships of G-protein coupled receptors. Issues like the actual mapping of the binding site of different subtypes, as well as the mechanism of activation are poorly understood [1]. Accordingly, further studies on the structure-activity relationships are necessary. In this regard, only a few 3D structures are available from X-ray diffraction studies. Computational studies can complement this information through the construction of reliable 3D models.

The goal of the present work is to evaluate the effect of using different ligands to obtain reliable models of the three-dimensional structure of a G-protein coupled receptor using a specific template. Specifically, we have constructed in the present work a three dimensional model of the M3 muscarinic receptor by homology modelling, using the X-ray structure of M2 muscarinic acetylcholine receptor as template and the sequence analyses of muscarinic acetylcholine receptor family. Furthermore, we have studied the effect of the ligand used in the modelling process. For this purpose three models of the receptor were built, including one without ligand and two models with the selective antagonists tiotropium and N-Methylscopolamine, respectively docked into the orthosteric binding site.

The constructed models were refined using molecular dynamic calculations to analyze the effect of ligand refinement process and to derive significant conformational information. Based on the analysis of the refined models done through the calculations of RMSD, RMSF, visualization of the structures and comparison between the refined models and the crystal structure of M3 muscarinic receptor, the addition of a ligand in construction of homology model (and the subsequent refinement process) stabilize the structure. Furthermore, the similarities in the structure conformations of both refined models of M3 muscarinic-ligand complexes and the crystal structure of the M3 muscarinic receptors, suggest that the methodology used in this study can be used in prediction of 3D structure prediction GPCR in the absence of crystal structures.

Chapter 1: Introduction

1.0. Introduction

The goal of the present master's thesis is to evaluate the effect of using different ligands to obtain a reliable model of the three-dimensional structure of a G-protein coupled receptor using a specific template.

Our approach to obtain reliable 3D models of G-protein coupled receptors (GPCRs) consists of constructing an initial model based on a template, selected from one of the solved crystal structures as close as the receptor being modelled and then, being refined using molecular dynamics. However, this approach presents several questions that requires a deep study: length of the simulations, choice of the template and the use of a ligand or not during the refinement process.

In the present work we have analyzed the effect of the ligand in the modelling of the M3 muscarinic receptor using the M2 muscarinic receptor as template. Three models were constructed and compared to the M3 crystal structure: a model with no ligand inside, together with two models using two different antagonists, tiotropium and N-methylscoplamine.

1.1. G-protein coupled receptors superfamily

GPCRs constitute a large family of integral proteins that are activated by foreign molecules or other stimuli, binding to the outside region of the cell triggering a signal transduction pathway inside the cell that finally produces a cellular response. These receptors are embedded in the cell membrane and exhibit a conserved seven transmembrane helix bundle structure connected by three extracellular and three intracellular loops with the N-terminus located at the extracellular domain.

This family of receptors -the largest family of integral proteins- contains about 8200 membranes and are expressed by roughly 3% of genes in the human genome [2]. They regulate virtually all known physiological process in mammals and humans, being also found in prokaryotic cells, including yeast or choanoflagellates [3].

GPCRs play an important role in many diseases and, also are the target of approximately 60% of all modern medicinal drugs [4-9], which contrasts to the small proportion of genes in the human genome that are predicted to encode GPCRs, illustrating the importance of these proteins both medically and pharmaceutically. They are implicated in a number of illnesses on the human genomes, as some studies shows, vast number of mutations have

been identified in GPCRs (both activating and inactivating) which are responsible for more than 30 different human diseases [10], such as cancer [11, 12], diabetes [13], hyperthyroidism [14], ovarian hyper stimulation syndrome [15, 16], congenital stationary night blindness [17] as well as being implicated in causing obesity [18].

Activation of GPCRs can activate different transduction mechanisms, including control of enzyme activity, activation of ion channels or vesicle transport, responding to the wide range of different stimuli, such as sensory signals, hormones and neurotransmitters. There are many ligands that bind to this kind of receptors and active them to provoke different physiological responses. Ligands include light-sensitive compounds, odors, pheromones, hormones, and neurotransmitters and are different in size and dimension from small molecules to peptides and finally large proteins.

Upon binding of an agonist GPCRs change conformation (in actuality the population of the activated conformation increases) allowing the interaction with a heterotrimeric G protein, consisting of three distinct subunits, termed α, β and γ. The interaction of agonist activated receptor with the G protein receptor provokes a dissociation or at list loss of association of the α subunit from the β, γ subunit dimer, that permits that both the α subunit and the β, γ subunit can independently activate different downstream signaling proteins.

To further understand the molecular mechanism underlying diseases and the syndromes caused by mutations related with these receptors, as well as for the design of small molecules acting as therapeutic treatments, a deeper understanding of the structure activity relationships is necessary.

Currently, there is an enormous activity in obtaining three dimensional structures of GPCRs from X-ray diffraction studies. This is in part due to the pioneering efforts of Kobilka and Leftkowitz devoted to study the structure and function of these proteins, considered by the Nobel committee as "crucial for understanding how G-protein– coupled receptors function" [19] who awarded them with the Nobel Prize in chemistry of 2012 for their studies.

Although there are a number of structures available, including rhodopsin [20, 21], β-1 adrenergic receptor [22], β-2 adrenergic receptor [4, 23], adenosine A2a receptor [24] and others released more recently, computational methods are frequently used to facilitate the identification and characterization of novel receptors and their structures. Nowadays

computational methods are seems to be most powerful methods when combined with high-throughput testing of rationally designed molecules and experimental data in the laboratories.

1.1.1. Classification of the GPCR superfamily

Although all GPCRs belong to one superfamily, sequence alignments of GPCRs show that identity is not overall, but concentrated in the segments related to the transmembrane regions. On the basis of these alignments, several conserved residues in the 7TM bundle were identified. Moreover, analysis of the alignments show that GPCRs can be subdivided into families on the basis sequence homology and/or pharmacological characteristics as can be seen in figure (1.1). Families can be classified according to their receptor-ligand interactions.

- Class A (or 1) (Rhodopsin-like)
- Class B (or 2) (Secretin receptor family)
- Class C (or 3) (Metabotropic glutamate/pheromone)
- Class D (or 4) (Fungal mating pheromone receptors)
- Class E (or 5) (Cyclic AMP receptors)
- Class F (or 6) (Frizzled/Smoothened) [25-28]

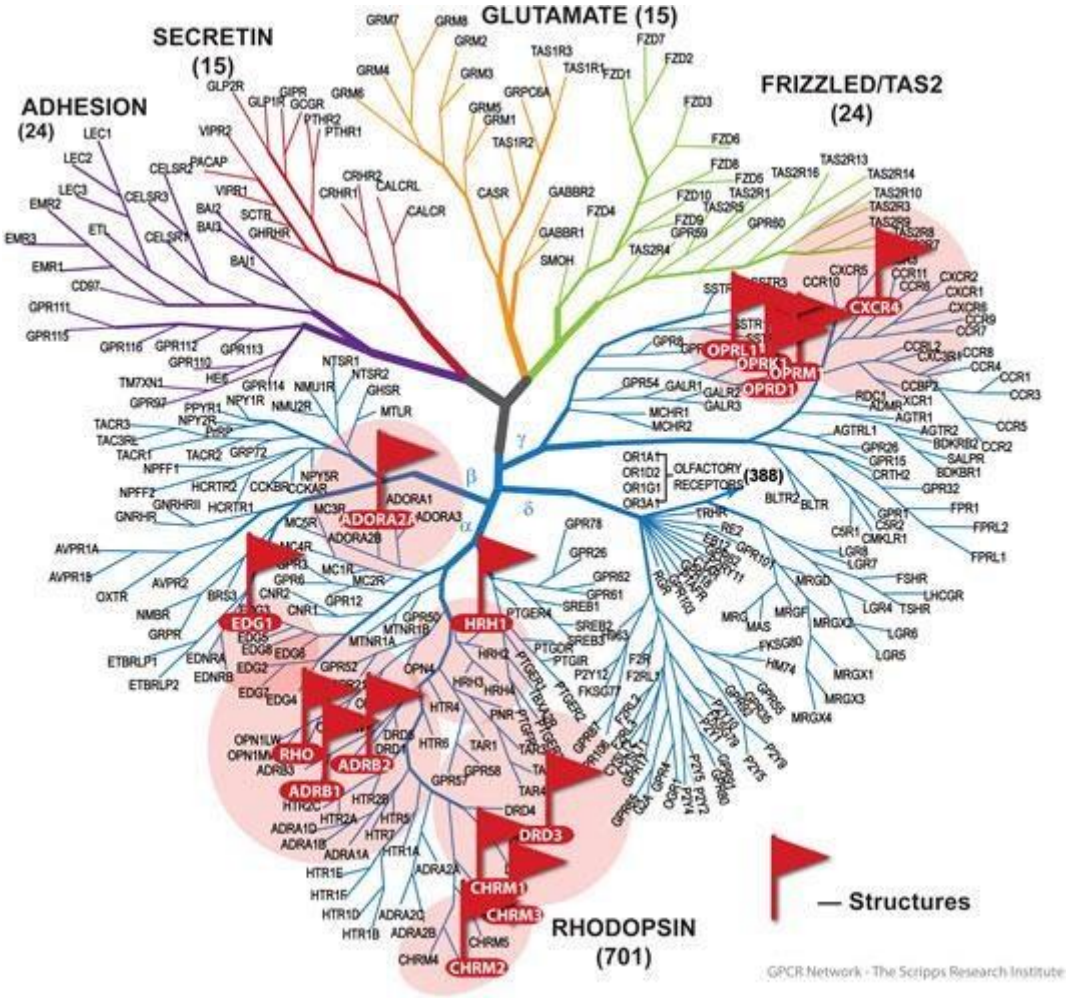

Figure (1.1): Classification scheme of GPCRs. Class A (Rhodopsin like), Class B (Secretin like), Class C (Glutamate Receptor like), Others (Adhesion), Frizzled, Taste typ-2, unclassified [29]

The largest family in this classification is rhodopsin like (family A), which give importance to this particular membrane of GPCRs.

1.1.2. 3D structure of GPCRs belonging to the Family A

As mentioned above all members of the GPCR family exhibit similar features in their three-dimensional structure, consisting of a tightly packed bundle of seven transmembrane helices. The seven-membrane spanning domain putatively form a barrel oriented roughly perpendicular to the plane of the membrane, with an extracellular amino-terminus and intracellular carboxyl terminus, three connecting loops located in the extracellular space (ECL1-ECL2) and three located in the intracellular (see figure (1.2)). The extracellular parts of the receptor can be glycosylated. These extracellular loops in the family A receptors often contain two highly-conserved cysteine residues that form a disulfide bond to stabilize the receptor structure [30, 31].

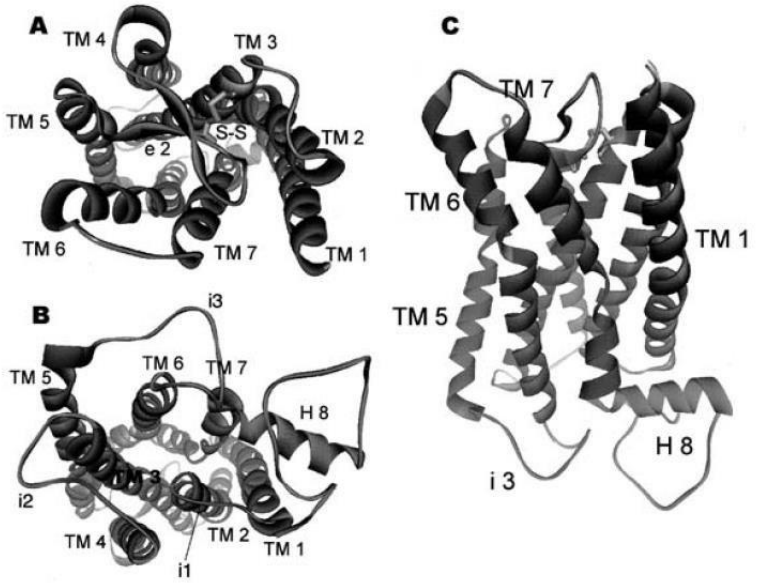

Figure (1.2): Homology model of the M1 mAchRs. (A) View from the extracellular side (e); (B) view from the intracellular side (i); (C) view from the TM domain [30]

However, despite numerous efforts only few proteins structure has been solved though X-ray diffraction studies. Rhodopsin was the first GPCR to be crystallized [32] and its structure was deduced from X-ray diffraction data at 2.65 Å resolution (PDB entry 1GZM). This milestone permitted an unprecedented advance in our understanding of the structure and activation of the family A of GPCRs. A few years later, the high resolution crystal structure of the β2 adrenergic receptor at 3.4 Å resolution was determined [33, 34]. This structure provided the opportunity to evaluate an actual ligand-mediated GPCR for its use in structure-based drug design. Moreover, the crystal structure of the human A2R adenosine receptor, in complex with a high-affinity subtype-selective antagonist, ZM241385 at 2.6 Å resolution was also determined [24]. Interestingly, four disulphide bridges in the extracellular domain, combined with a subtle repacking of the transmembrane helices relative to the adrenergic and rhodopsin structures were detected; defining a pocket distinct from that of other structurally determined GPCRs. More recently, the crystal structure of the CXCR4 chemokine receptor was published providing new insights of the structure of GPCRs. Other structures followed, including the M2 and M3 muscarinic acetylcholine receptors, which are members of the subfamily of muscarinic receptors (see part (1.2), β-1 adrenergic receptor, opioid receptor, histamine receptor and dopamine receptors.

1.2. Muscarinic receptors

The muscarinic acetylcholine receptors belong to the prototypic family A (rhodopsin like) GPCRs. Muscarinic acetylcholine receptors have many roles in activity of the neurotransmitter acetylcholine in the central and peripheral nervous systems. Depolarization of the nerve terminal causes an influx of calcium into the nerve terminal and evokes the release of acetylcholine into the synaptic cleft. Acetylcholine is synthesized in the cytoplasm of nerve terminals by the enzyme choline acetyltransferase, and is then transported into synaptic vesicle.

As can be seen in figure (1.3), acetylcholine acts at neuron-neuron and neuron-muscular cell synapses and binds to the cholinergic receptors: nicotinic and muscarinic, propose by Dale in 1914[35]. The former are Na+ and K+ channels, whereas the latter are GPCRs.

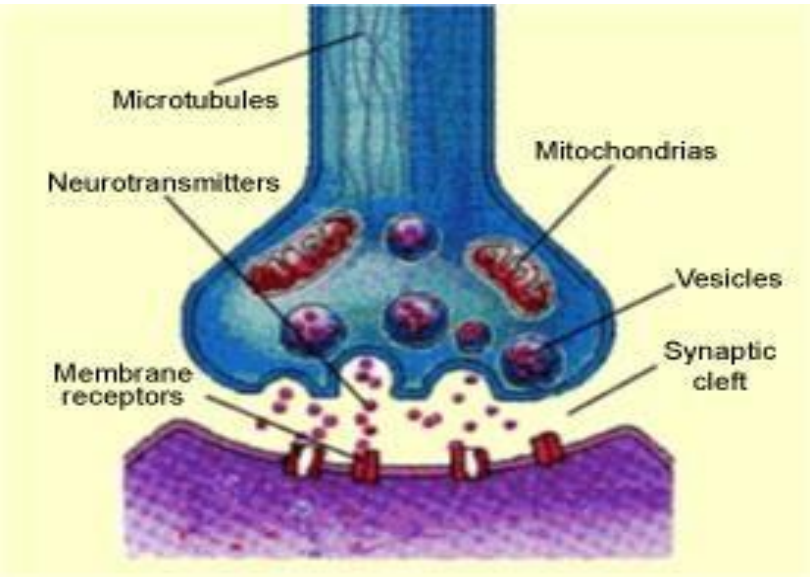

Figure (1.3): Action of acetylcholine at the muscarinic receptors, adapted from reference [35]

1.2.1. Common structural features of the muscarinic acetylcholine receptors

Muscarinic receptors like the rest of the members of the family A of GPCRs, exhibit a seven helix bundle with a ligand-recognition site which bind to small molecules. The first 3D structures of these receptors were constructed by homology modelling studies using the crystal structure of rhodopsin as template [36]. The main features of muscarinic receptor structure are included at table (1.1). The cytoplasmatic domains appear to contain important determinants for receptor/G protein interaction and are likely to contain sites agonist- and/or second messenger-dependent phosphorylation. Specifically, the third intracellular loop (i3) of GPCRs which confers specificity for G protein coupling [37]. In

muscarinic receptors as well as dopamine D2–4, adrenergic α2A–2C, and 5-hydroxytryptamine1A receptors, the i3 has been observed to be long (with more than 100 residues). In fact the number of residues in muscarinic subtype i3 is between of 160 and 240 residues.

Studies based on mutagenesis have shown that the N- and C-terminal portions of i3 play a key role in the specificity of the coupling of muscarinic receptors to G proteins. On the other hand, most of the central part of i3 can be deleted without impairing the ability of the M2 receptor to couple with G proteins, indicating that only the N- and C terminal portions of i3 are required for the interaction. Consistently, most GPCRs have a short i3 and lack its long central part. The question is raised if these long i3 loops have a common physiological function and similar tertiary structure, although their sequences are not similar [38, 39].

Table (1.1): Main feature of muscarinic acetylcholine receptors

NUMBERS	FEATURES
1	The transmembrane segments are likely alpha helices
2	The ligand recognition site is within the outer half of the membrane embedded part of the protein [40].
3	There are two conserved cysteine residues that form disulfide bound between the first and the third extracellular loops [41].
4	There is a conserved triplet of amino acids (DRY) at the cytoplasmic interface of TM3 with the second intracellular, which is important for both the expression and function of the receptor [42].
5	The carboxy-terminus is on the intracellular side of the membrane because antibodies to the C-terminus sequences recognize cell-surface receptors only when cells are permeabilized [42].

There is little known about the role of the extracellular receptor domains in the function of class A GPCRs that are activated by small diffusible ligands. In the case of the muscarinic receptors, the extracellular domains, specially the o2 loop, have been shown to play important roles in the binding of certain snake toxins which prevent the receptor activation by classic muscarinic agonists. Moreover, despite mutagenesis studies are not related to this study, but carry out mutagenesis study with different muscarinic receptor subtypes suggests that residues located within the o2 loop and other extracellular domains make critical contacts with allosteric muscarinic ligands [43].

In addition, recognition of common features of the muscarinic receptors, identifying difference among of muscarinic receptors subtypes is important for our study, since activation of the various subtypes of muscarinic acetylcholine receptors leads to different impacts on some parts of human body. Also, it cause to make better structure design by comparison with previous studies.

1.2.2. Muscarinic receptor subtypes

There are different subtypes of muscarinic acetylcholine receptors, characterized for binding specific ligands. Five subtypes of muscarinic acetylcholine receptors (M1-M5) have been recognized and discovered to be widely expressed in the central nervous system and in the peripheral tissues. In the CNS, there is evidence that muscarinic receptors are involved in motor control, temperature regulation, cardiovascular regulation, and memory [40]. They expose high sequence homology with each other and with other GPCRs with their seven transmembrane helices, whereas the sequences are more variable at the amino terminal extracellular region, lying at the entrance of ligand, and at the third intracellular loop. Specifically, the carboxyl-terminal end of the third intracellular loop of the receptor has been implicated in the specificity of G protein coupling. Activation of the different subtypes of muscarinic acetylcholine receptors leads to different effects, thus for example: M1, M3 and M5 receptors stimulate phosphoinositol metabolism, while M2 and M4 receptors inhibit adenylatecyclase pathway [44].

Cloning of the five mammalian genes encoding the muscarinic receptors, was carried out by Ishii and Kurachi in 2006 [45]. The expression of different subtypes in cell lines resulted in the generation of useful information about their structure-function relationships. Their result which are shown in the Table below, illustrate that there are many agonists and antagonists for the muscarinic receptors. Some of them are selective for certain receptor subtypes and are often used as pharmacological tools for analyzing and explaining the function of the individual muscarinic acetylcholine receptors:

Table 1.2. Muscarinic receptor subtypes and their pharmacology [45].

	M1R	M2R	M3R	M4R	M5R
Non selective agonists	Acetylcholine (muscarinic and nicotinic), Carbachol (muscarinic and nicotinic), Muscarine (muscarinic receptor specific), Pilocarpine (muscarinic receptor specific), Oxotremorine-M (muscarinic receptor specific), Metoclopradime (muscarinic receptor specific), Bethanechol (muscarinic receptor specific)				
Non selective antagonists	Atropine, Scopolamine, QNB (Quinuclidinyl- α-hydroxydiphenylacetate)				
Subtype selective agonist	McN-A-343 l-689,660 Xanomeline CDD-0097	-	L-689,660	-	-
Subtype selective antagonist	Pirenzepine Telenzepine MT7	AF-DX-116 AF-DX-384 Methoctramine Himbacine Tripitramine	4-DAMP Darifenacin	AF-DX-384 Tropicamide Himbacine	

Here, the M2 muscarinic receptor was chosen among different subtypes. As can see in table (1.2), one of the selective M2 muscarinic receptor antagonist is tiotropium, which is separated slowly from M3 muscarinic receptor in comparison with M2 muscarinic receptor (in part 1.4.1 we will discuss more about tiotropium).

1.2.3. The M2 muscarinic receptors

M2 muscarinic receptor is expressed through the central nervous system and in the periphery, in particular in smooth muscle and tissues of the heart. The M2 muscarinic receptors are responsible of the regulation of force and rate of heart beating. The M2 receptor appears to be exclusively responsible for these effects on heart beating regulation despite the presence of the other muscarinic receptor subtypes in heart cardiac muscle [40]. The muscarinic agonist carbachol induces bradycardia in spontaneously beating sinoatrial node cells and atria; an effect that was completely abolished in M2 receptor deficient mice, indicating that this receptor is responsible for cholinergic deceleration of the beating heart. This result was demonstrated through some related exams in M2 receptor-deficient mice. It is has been also demonstrated that the receptor plays a crucial role in muscarinic agonist-induced amnesia [46]. On the other hand, electrophysiological examination showed that the muscarinic receptor dependent inhibition of the neuronal (N and P/Q type) calcium channel was abolished in sympathetic ganglion neurons from M2 receptor-deficient mice. In these mice, the carbachol-mediated contraction of a smooth muscle preparation was slightly attenuated [47].

1.2.4. The M3 muscarinic receptor

Within the muscarinic family, the M3 subtype mediates many important physiological functions, including smooth muscle contraction and glandular secretion. The muscarinic M3 receptor is settled mainly in smooth muscles and salivary glands. Therefore, the M3 selective antagonists have therapeutic potential in the disorders therapy deal with altered smooth muscle contractility or tone, including chronic obstructive airway disease, urinary incontinence, and irritable bowel syndrome [48-53]. The M3 receptor is found in high levels in neuronal cells of the CNS; its distribution largely overlaps with that of m1 and m4 subtypes. It is also found in peripheral ganglia, exocrine glands, Smooth muscle, vascular endothelium, and in cell lines. No selective agonist has been described [54]. Recently, the role of the M3 receptor in insulin secretion was emphasized [55].

Expression of M3 muscarinic receptor is found in different part of body such as brain (smaller expression than M2 and M1 muscarinic receptor), smooth muscle and glandular tissue [56]. Central M3 receptors have also been implicated in the regulation of food intake, learning and memory, and the proper development of the anterior pituitary gland Selective drugs targeted at this receptor subtype may prove clinically useful.

Knock-out mice lacking the M3 muscarinic receptor exhibit a remarkable (~25%) reduction in body weight as well as a significant reduction (~40-95%) in carbacholinduced contraction of smooth muscle (urinary bladder, ileum, stomach fundus, trachea and gallbladder). Moreover, these mice show no carbachol induced contraction of smooth muscle in urinary bladder, in contrast of the effect on the M2 muscarinic receptor-knockout mice, suggesting the crucial role of the M3 receptor for inducing contraction in this tissue [57].

Clearly, the M3 muscarinic receptor subtype performs multiple physiological actions and it is implicated in numerous pathological conditions. Because of the significant role of the M3 receptor in different diseases, it is the main subtype that its structure is investigated (figure 1.4)

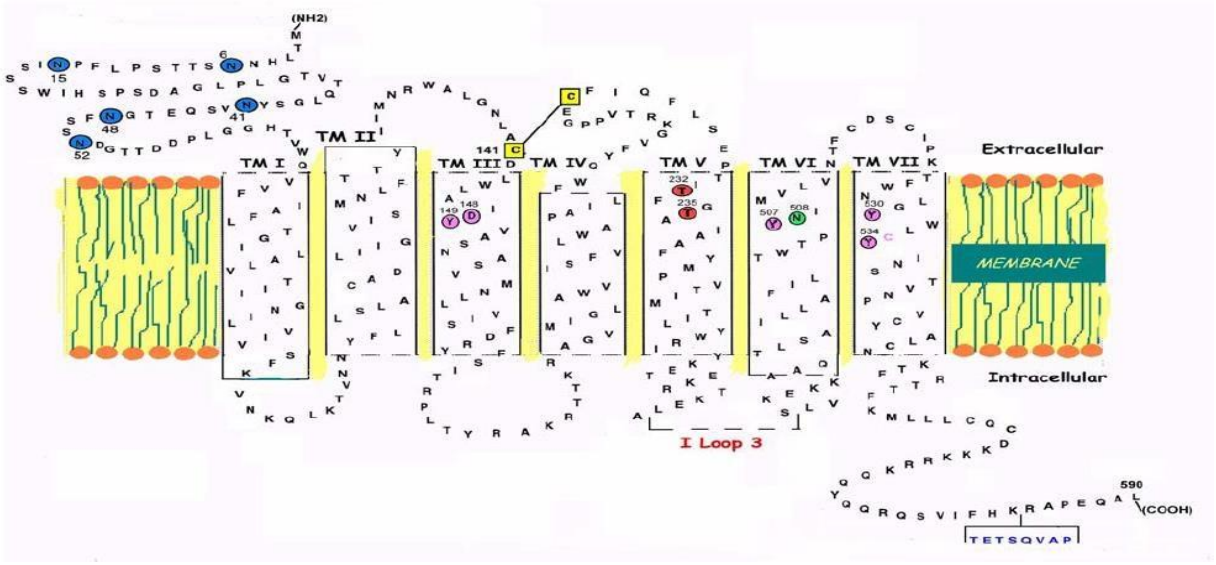

Figure (1.4): Secondary structure of human M3 muscarinic receptor. In blue the N methylglycosilation of the N-terminus, in yellow the cysteine bridge between Cys 141- Cys 221, in red, purple and green the residues of the binding pocket. In the C-terminus, it is shown a box with nine residues (in blue) corresponding to the C terminal epitope of bovine rhodopsin that is recognized by the monoclonal antibody 1D4 [58]**.**

1.2.4.1. Important residues of the M3 muscarinic receptor involved in the interaction with ligands

3D models of receptors are useful to understand the structure–activity relationship (SAR) [59, 60]. SAR analysis enables the determination of the chemical groups responsible for evoking a target biological effect in the organism. This allows modification of the effect or the potency of a bioactive compound (typically a drug) by changing its chemical structure. Medicinal chemists use the techniques of chemical synthesis to insert new chemical groups into the biomedical compound and test the modifications for their biological effects [25].

Besides a quaternary or protonated amine head group, all strong muscarinic agonists and antagonists consist of one or more polar functional groups such as ester, ether or amide moieties that are capable of participating in hydrogen bonding interactions [61].

Based on the this fact that an asparagine residue present in transmembrane domain I of all muscarinic receptors is critically involved in the binding of the acetylcholine ester moiety by means of hydrogen bonding. Bluml et al. [58] designed several mutants of the M3 muscarinic receptor in which residue Asn507 was replaced with alanine, serine, or aspartic acid. Their data suggest that the asparagine residue present in transmembrane domain VI of all muscarinic receptors is not critical for acetylcholine binding and agonist-induced receptor activation, but plays a key role in the binding of certain subclasses of muscarinic antagonists [62].

Mutagenesis as well as peptide labeling and sequencing studies of adrenergic [63-65] and muscarinic receptors also suggest that the binding of agonists and antagonists is initiated by an ion -ion interaction between the amine moiety of the ligands and an Aspartic acid residue located in TM3 of the receptor proteins. Since this residue is conserved among all receptors which bind biogenic amine ligands such as the adrenergic, dopamine, serotonin, muscarinic and histamine receptors, the specific binding of a particular amine ligand to a given receptor must be accomplished by additional mechanisms such as hydrogen bonding interactions.

Conspicuously, the hydrophobic core of all muscarinic receptors contains a series of conserved serine, threonine and tyrosine residues which with very few exceptions, do not occur in any other G-protein linked receptor. In order to test their potential involvement in specific binding of muscarinic ligands, Wess et al. [37] mutated these residues by alanine in the case of serine and threonine or by phenylalanine in the case of tyrosine, using the rat M3 muscarinic receptor. Ligand binding and functional properties of the various mutant receptors were determined after their transient expression in COS7 cells. Interestingly, six amino acid residues were identified which appear to be critical for agonist binding but are of little or no importance for antagonist binding. Results show that among them the mutant M3 muscarinic receptors which showed the strongest decreases in agonist binding affinities (30- to 40-fold lower than the wild-type receptor) were Thr234Ala and Tyr506Phe. The hydrogen bonding interactions between Thr234 and Tyr506 and muscarinic agonists may therefore cause conformational changes in these two transmembrane domains which could be transmitted to the connecting loop resulting in the activation of specific G proteins [66].

Despite the muscarinic M3 receptor has been widely studied, the binding mode of the ligands is still ambiguous [67]. Until now, various agonists and antagonists of the muscarinic M3 receptor have been disclosed, but most of them show little selectivity for the M3 receptor. To design selective and potent M3 ligands as potential candidates for clinical trials, computational methods are currently used. The present work investigates the interactions of human muscarinic M3 receptor and its ligands by means of a combined ligand-based and target based approach, consisting of homology modeling of the hM3 receptor and docking of representative ligands such as tiotropium and NMS. Interactions of antagonist with M3 muscarinic receptor occurs in orthosteric binding site which is described in next part.

1.3. The orthosteric binding site of GPCRs

Binding of agonists and competitive antagonists to GPCRs occurs at the orthosteric site, a hydrophobic pocket which is placed at the extracellular side of the helix bundle that is highly conserved among the members of a subfamily [39, 68]. Interestingly, while residues defining the orthosteric binding site are well conserved within the different GPCR subfamilies, those of the extracellular loops are remarkably diverse within a subfamily, providing a good possibility to design selective allosteric antagonist [69]. Broadly knowledge of the structure-activity relationships of the different subtypes will help designing new selective ligands with various pharmacological profiles that may be beneficial for therapeutic intermediation. In this sense, due to the scarcity of crystallographic structures available, molecular modeling methods can provide a deeper insight into the flexibility and the role that extracellular loops may play in ligand recognition [70].

1.4. Muscarinic receptors antagonists

A receptor antagonist is a type of receptor ligand or drug that does not provoke a biological response itself upon binding to a receptor, but blocks or dampens agonist mediated responses. Residues important for the binding of ligands have not been defined. Sites involved in binding different receptor-selective antagonists are probably quite diverse, depending on the antagonist [57]. It is very difficult to identify amino acids that interact directly with antagonists and to distinguish such residues from those which, when mutated, affect antagonist binding site suggested that a conserved Asn residue in the sixth transmembrane segment is very important for the binding of certain subclasses of antagonists [62] that in this study tiotropium and N-methylscoplamine are our interest antagonist to follow aim of the investigate.

1.4.1. Tiotropium

Tiotropium is a specific antagonist (long-acting, 24 hour, anti-cholinergic bronchodilator)of muscarinic receptors that binds to all receptor subtypes with similar affinity (figure 1.5), but it dissociates from the M1 and M3 muscarinic receptors more slowly than from the M2 muscarinic receptor. Also it often referred to as an antimuscarinic or anti-cholinergic agent. In contrast to ipratropium, tiotropium has roughly a tenfold greater affinity for muscarinic receptors, and it dissociates ~100-fold more slowly from the M1 and M3 muscarinic receptors, because of the rationale behind

the sustained bronchodilation obtained with tiotropium. On tropical application it acts mainly on M3 muscarinic receptors [71, 72] located on smooth muscle cells and submucosal glands leading to a reduction in smooth muscle contraction and mucus secretion, thus producing a bronchodilatory effect. This translates into a prolonged duration of action for tiotropium bromide compared with ipratropium bromide, allowing once-daily dosing via oral inhalation.

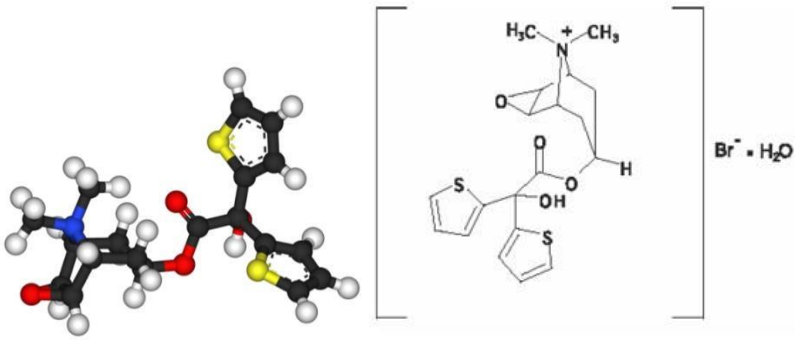

Formula $C_{19}H_{22}BrNO_4S_2$

Figure (1.5): structure of tiotropium

Tiotropium is used for maintenance treatment of chronic obstructive pulmonary disease (COPD) which includes chronic bronchitis and emphysema [73]. It is not however used for acute exacerbations [43]. In chronic obstructive pulmonary disease (COPD) and asthma, inflammatory conditions lead to loss of neuronal inhibitory activity mediated by M2 on parasympathetic nerves, causing excess acetylcholine reflexes [74] which result in airway hyper reactivity and hyper responsiveness mediated by increased acetylcholine release and thus excess stimulation of M3. Therefore, potent mAchRs antagonists, particularly directed toward the M3 subtype, would be useful as therapeutics in these muscarinic acetylcholine receptor mediated disease states [75], mostly through activation of the human muscarinic M3 receptor (hM3) subtype [4].

1.4.2. N-Methylscopolamine

N-Methylscopolamine (NMS) is a methylated derivative of scopolamine, and a muscarinic antagonist structurally similar to the neurotransmitter acetylcholine. Its mechanism of action involves blocking the muscarinic acetylcholine receptors.

Methylscopolamine or meth scopolamine, usually provided as the bromide salt (trade name Pamine), is an oral medication used along with other medications to treat peptic ulcers by reducing stomach acid secretion. With the advent of proton pump inhibitors and antihistamine medications it is rarely used for this anymore. It can also be used for stomach or intestinal spasms, to reduce salivation and to treat motion sickness. Meth scopolamine is also commonly used as a drying agent, to dry up post-nasal drip, in cold, irritable bowel syndrome and allergy medications.

In a recent investigation an optimized rhodopsin-based homology model of the muscarinic receptor M_1 has been used to dock NMS and other ligands, in a manner compatible with the effects of the TM domain alanine mutations on binding affinity. They suggest that at the bottom of the binding pocket of the muscarinic M_1 receptor, mutagenesis and modeling suggest that Trp378 contributes directly to the binding pocket for NMS although possibly with different side chain orientations [76] (figure 1.6)

As mentioned above, the precise binding of ligands is largely unknown and every ligand has its particular binding. At the M3 muscarinic receptor the mutation of tryptophan 6.48 to phenylalanine reduces NMS affinity [37]. Thus, the aromatic character of Trp378 may be key for the binding of NMS. Moreover, molecular modeling studies suggest that the side chains of NMS follow distinct vectors within the binding site (Figure 1.5). The phenyl ring of the tropic acid side chain of NMS may extend deep into the transmembrane domain region toward TM5 [76].

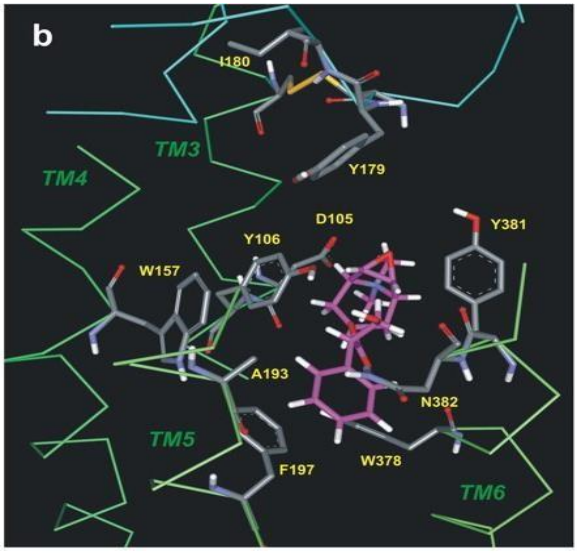

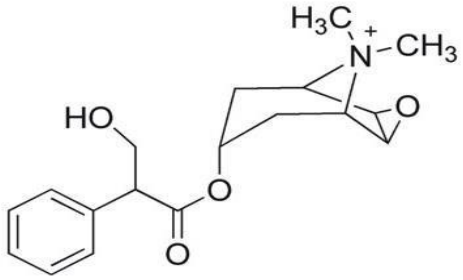

NMS

Figure (1.6): Molecular model of the muscarinic M_1receptor binding site docked with N-methylscoplamine [76].

Chapter 2: Methods

2.0 Computational chemistry

Computational chemistry concerns the utilization of analytical (data) and theoretical methods, mathematical modeling and computational study of biological, chemical and behavioral systems. There are two fields of computational chemistry: information management and molecular modeling. The former refers to the management and analysis of huge amounts of data created by combinatorial chemistry and genomic sequencing. On the other hand, molecular modeling consist in the construction of a mathematical model that can be used to predict, explain and stimulate the behavior of a molecular system [61, 77, and 78].

In general, computational chemistry and molecular modeling can be used indistinctly, however it is important to keep in mind that molecular modeling does not always happens in a computer or using a computer and on the other hand, computational chemistry is not always about constructing models. Indeed, one can use a molecular modeling kit to build a physical model that represents molecules and their interactions [61, 77, and 78].

One the basic principles of medicine chemistry is that biological activity dependents on the three dimensional placement of specific functional groups that define a pharmacophore. Construction of a pharmacophore can be carried out in a ligand based manner, by superposing a set of active molecules and extracting common chemical features that are essential for their bioactivity, or in a structure-based manner, by probing possible interaction points between the macromolecular target and ligands [59, 60, 79-81]. Methods used in molecular modeling are related, and are not only restricted to the analysis of three dimensional structures. Thus, construction of protein models by sequence homology or molecular docking are also some other parts of the model construction. In molecular modeling different strategies are used to explore and deduce information of a system. Some of the strategies involve computation of the energy of a molecular system and energy minimization (calculating local energy minima) [80].

Some of the constructed molecular models utilize accessible crystallographic data.

Crystal structures are frequently as close as you can get to ‘reality’, but on the other hand, they are models and should be treated with some skepticism. The raised problem comes from multiple crystal structures of molecule (s) of interest which are available. In this situation, the higher resolution crystal structure is generally preferred. Among the high resolution crystal structures, the best one for docking is that one which does not have

missing portions, and which is preferably also unencumbered by the presence of a whole lot of counterions, stabilizing molecules, and other ligands [82, 83].When there is no crystal structure available, other methodologies may be applied like homology modeling [84-86]. After construction target protein or complex structure, the bonding of the compound of interest can be generated using a docking algorithm.

2.2. Homology Modeling

As mentioned in the previous section, characterization of a protein sequence is one of the most frequent problems in biology this task is usually facilitated by a three dimensional (3D) structure of the studied protein [87]. In other words, structure-activity studies require a high-quality three dimensional structure of the target receptor. Due to the difficulties associated in growing crystals for GPCRs, models of this class of proteins are currently constructed by homology modeling. This is an important issue, since homology models have application in virtual screening studies, docking experiments (small molecule and protein-protein interactions) as well as being used to generate hypotheses about intra- and inter-molecular mechanisms [88].

Homology modeling has become increasingly common and although any methods of homology modeling include of four sequential steps:

I. Template recognition
II. Alignment of the target sequence and template structure(s)
III. Model building
IV. Model verification, which may be used iteratively with steps i-iii.

Sequence alignment can be used to understand sequence similarity between template and target sequences, in particular in loop region that need high amount of alignment in both sequence and structure. [89].

The most probable arrangement of the seven helixes in GPCRs, was derived from structural information extracted from a detailed analysis of the sequence. These constraints include:

1. Each helix must be positioned next to its neighbors in the sequence.
2. Helices I, IV and V must be most exposed to the lipid surrounding the receptor and helix III least exposed.

3. Is established from the lengths of the shortest loops.
4. Is determined by considering: (i) sites of the most conserved residues; (ii) other sites where variability is restricted; (iii) sites that accommodate polar residues ;(iv) sites of differences in sequence between pairs or Within groups of closely related receptors[36].

2.2. Molecular docking

The aim of molecular docking is to computationally simulate the molecular recognition process. The associations between biologically related molecules such as proteins, nucleic acids, carbohydrates and lipid play a central role in signal transduction. Thus, the relative orientation of two interacting partners may affect the type of signal produced (e.g., agonist vs. antagonist). Because docking is helpful for predicting both the strength and type of signal produced. The purpose of molecular docking is for access an optimized conformation for both the protein and ligand and relative orientation between them, to know better the ruling principles whereby protein receptors recognize, interact and associate with molecular substrates and inhibitors is of paramount important in drug discovery attempts [90]. Protein-ligand docking leads to predict and rank the structures come from the dependency between a given ligand and a target protein of known three dimensional structure.

The capability to produce the binding poses is as important as the ability of its scoring function to score and rank ligands according to their experimental binding affinities. There have been a number of attempts for comparison strength of different docking protocols, where the comparison is often categorized into evaluation of the search algorithm and the scoring function [90-93]. A disinterested comparison of each effort obviously explained that it is very difficult to rank and recognize different optimization strategies, particularly with enhanced algorithms complexity. It was necessary to note that the implementation of any docking protocol with only depend on the core algorithms, the time invested in parameterization and optimization of the methodology.

There are several molecular docking software such as: Gold, Glide, Auto dock, etc. [9094] . In this study two pieces of software's were used: Genetic optimization for ligand docking (GOLD) and molecular operating environment (MOE).

2.2.1. Genetic optimization for ligand docking (GOLD)

Gold application is based on a genetic search algorithm that allows full ligand flexibility, as well as local flexibility for the protein receptor polar hydrogens [90, 91, 95, and 96]. Gold scoring function includes the analysis of about 100 different protein complexes and provides a 71% success rate in identifying the experimental binding models. However systemic problems in ranking have different polar ligands and in ranking general ligands in large cavities have been reported [16, 80, 97, and 98].

Like all docking program GOLD has three main parts:

1-ligand placement mechanism

2-search algorithm (conformational search)

3-scoring function

The first part of GOLD is the mechanism for placing the ligand in the binding site. GOLD ligand assignment is based on fitting points. The program adds fitting points to hydrogen binding groups on protein and ligand, and maps acceptor points in the protein and vice versa. Moreover, GOLD creates hydrophobic fitting points in the protein cavity onto which ligand CH groups are mapped.

The second part of GOLD software is the search algorithm to explore possible binding modes; GOLD applies a genetic algorithm (GA) in which the following parameters are modified /optimized:

- Dihedral of ligand rotatable bonds.
- Ligand ring geometries (by filliping ring corners)
- Dihedrals of protein OH groups and NH3 groups
- The mapping of the fitting points (i.e., the position of the ligand in the binding site) [16, 98].

Lastly a scoring function ranks different binding modes, the Goldscore function is a molecular mechanics –like function with four terms:

GOLD fitness=shb _ext +svdw_ext +shb_int Eq (2.1)

Where;

- **Shb_ext** is the protein -ligand hydrogen bond score.
- **Svdw_ext** is the protein -ligand van der Waals score.
- **Shb_int** is the contribution to the fitness due to intramolecular hydrogen bonds in the ligand.

- **Svdw_int** is the contribution due to intramolecular strain in the ligand [16, 98].

In this study GOLD software was used to perform the main docking calculations, using the Goldscore as a scoring function and the parameters chosen includes flipping ring corners ,planer and pyramidal nitrogen ,allowing ratable H2O molecules, diverse poses during placing and rotating interacting hydrogen bonds .

2.2.2. Protein and ligand preparation using MOE

MOE[1] is a software system designed to support among other things molecular modeling, and structure -based -design. Using the SVL (scientific vector language), a scripting and application development language of MOE, can be used as a platform with another program .In this study MOE was used at the stage of preparation of molecular structures, energy minimization, post docking refinement and visualization.

Molecular system optimization involves preparing the structure to be docked for the stimulation .in the case of this study, it included identification of missing residues and atoms, energy minimization and protonation states assignment. Unfortunately, most macromolecules crystal structure contain little or no hydrogen coordinates data due to limited resolution or disorders in the crystal. Explicit hydrogen atoms are required for all atoms molecular mechanics, docking and electrostatic calculations. The initial state of the hydrogen bond network and ionization state of treatable groups can have a dramatic effect on docking results.

Since the hydrogen data is missing in PDB files most software programs assign default protonation states to amino acid, or nucleic acid residues as well as counter ions and other solvent, the additional of hydrogen atoms to the macromolecules is a non-trivial task .MOE uses Protonate 3D method to do this. The purpose of the Protonate 3D function is to assign ionization states and position of hydrogens in macromolecular structure given in 3D coordinates (typically from a crystal structure). The main task is to determine;

- The rotamers of –SH –OH –CH3 and –NH3 groups in Cys, Ser,Tyr,Thr,Met and Lys;
- The ionization states of acids and bases in Arg,Asp,Glu,Lys,His ;

[1] http://computing.scs.illinois.edu/sites/default/files/SCS-UIUC-moe-tutorial-dock-05-2011.pdf

- The tautomers of imidazoles (His) and carboxile acids (Asp,Glu). The protonation state of metal ligand atoms Cys,His,Asp,Glu,etc ; The ionization state of metals.
- The element identities in His , terminal amides (Asn,Glu) and sulfonamides; The orientation of each water molecule.

Afterward the missing residue and atoms added to the receptor structure as well as the ligand structures were submitted to an energy minimization calculation .energy minimization is necessary to provide a local energy minimum, lower energy states are more stable and thus are considered to be the native state of the system. For this study the MOE's MMFF94x force field was used .it should be noted that a good force field is able to quantatively describe the ligand and the target individually as well as bound. This requires the force field to have outstanding prediction of conformational energies and good prediction of molecular geometrics if it is to avoid modeling the wrong conformations of ligand or receptor upon binding or providing a poor estimate of energetic cost of adapting the detailed conformation required for binding. MMFF94x is the best force field for computing behavior of small molecules, protein and nucleic acid structures, Furthermore, MMFF94x is particularly distinctive in its performance when applied to studies of binding [99].
The objective of this thesis is to study the muscarinic M3 receptor by molecular dynamics simulations therefore we decided use the M3 muscarinic receptor model to develop the molecular dynamics simulations.

Molecular Mechanics (MM) and Molecular dynamics (MD) are related but different. Main purpose of MD is modeling of Molecular Dynamics molecular motions, although it is applied for optimization. Molecular Mechanics and Molecular Dynamics are usually based some classical force fields.

2.3Molecular dynamics Simulations

Molecular dynamics (MD) simulations is a powerful technique to obtain detailed information on the structure and dynamics of macromolecules. Specifically, it provides atomic-level insights into variety of systems of increasing size and complexity, including the simulations of 7-transmembrane protein embedded in membranes [100].

Molecular dynamics simulations generate information at the microscopic level, including atomic positions and velocities, through microscopic simulations. The conversion of this

microscopic information to macroscopic observables such as pressure, energy, heat capacities, calculate changes in the binding free energy of a particular drug candidate, or to examine the energetics and mechanisms of conformational change, requires statistical mechanics. Statistical mechanics is fundamental to the study of biological systems by molecular dynamics simulation, which provides the rigorous mathematical expressions that relate macroscopic properties to the distribution and motion of the atoms and molecules of the N-body system; molecular dynamics simulations provide the means to solve the equation of motion of the particles and evaluate these mathematical formulas. With molecular dynamics simulations, one can study both thermodynamic properties and/or time dependent (kinetic) [101]

Nowadays MD simulations have the power to gain insight into different kinds of chemical reactions at atomic level. Therefore the MD simulation technique has become quite powerful in elucidating features of biological macromolecules.

Examples of commonly used programs for MD simulations biomolecules are AMBER [102], CHARMM [103], ENCAD [104] and GROMOS. The major packages have similar capabilities in terms of what systems can be studied and the kinds of your molecular system, the actual simulation has to be performed and finally the results have to be analyzed.

2.3.1 MD principles

Using MD it is possible to stimulate the time-evolution of a molecular system, which is represented classically considering a set of particles defined by their positions and momenta.

Molecular dynamics simulations are based on solving Newton's second law or the equation of motion. Newton's equation of motion is given by:

$$F_i = m_i a_i$$

Where F_i is the force exerted on particle i, m_i is the mass of particle i and a_i is the acceleration of particle i. From knowledge of the force on each atom it is possible to determine the acceleration of each atom in the system. The method is deterministic, once the positions and velocities of each atom are known; the state of the system can be predicted at any time in the future or past.

The force of an atom can also be expressed as the gradient of the potential energy,

$$F_i = -\nabla_i V$$

The potential energy is a function of the atomic positions of all the atoms in the system. Combining these two equations it yields:

$$-\frac{dV}{dr_i} = m_i \frac{d^2 r_i}{dt^2}$$

Where *V* is the potential energy of the system. Newton's equation of motion relate the derivative of the potential energy to the changes in position as a function of time. Due to the complicated nature of this function, it must be solved numerically. Numerous numerical algorithms have been developed for integrating the equations of motion such as: the Verlet algorithm, Leap-frog algorithm, velocity Verlet or the Beeman´s algorithm.

2.3.2 Force fields

The accuracy of the energy function directly affects the stability of MD simulations of biological macromolecules. For reasons of computational efficiency when dealing with large macromolecular systems the energy function has to be simple, and since force calculations are needed in MD simulations, the function should also be analytically differentiable.

Force field refers to the functional form and parameter sets to describe the potential energy of a system of particles. The basic functional form of a force field encapsulates both bonded terms relating to atoms that are linked by covalent bonds, and non-bonded terms describing the long-range electrostatic and van der Waals forces. The specific decomposition of terms depends on the force field, but a general form for the total energy in an additive force field can be written as:

$$E_{total} = E_{bonded} + E_{nonbonded}$$

The intramolecular potential energy is typically represented by harmonic oscillators for bond stretching and angle bending, a Fourier series for each torsional angle, and Coulomb and Lennard-Jones (LJ) accounting for the interactions between atoms separated by three or more bonds. The latter two terms –referred together as non-bonded terms- are evaluated between all atom pairs in the system to yield the intermolecular energy. Such force fields compute the energy as a sum of terms representing bond elongation, angle and dihedral deformation, and non-bonded interactions with the following general form:

$$E = \sum_{Bonds} V^{str} + \sum_{angles} V^{bend} + \sum_{torsions} V^{tors} + \sum_{LJ} V^{LJ} + \sum_{Coulumb} V^{Coul}$$

Where the first three summations correspond the bonded terms (that include atoms connected up to three consecutive bonds) and the last two refer to the non-bonded ones. All summations can be easily calculated from the coordinates of the system at a given time.

There are four main force fields in common use for simulation biological macromolecules: AMBER [105], CHARMM [103] GROMOS and OPLS [106]

The all-atom OPLS force field [106] which implemented in GROMACS was used for all molecules of the system [107]. OPLS refers to Optimized Potentials for Liquid Simulations. This force field have proved to be highly successful in computing liquid state thermodynamic properties and more recently in protein and protein-ligand modeling. Although non-bonded interactions (charge-charge and van der Waals terms) can be obtained from liquid state calculations, Parameters such as stretching, bending and torsional terms are generally fit to quantum chemical calculations. So they can be superior to many alternatives.

The components of the systems studied included proteins, lipids, water molecules and ions were as follows:

Protein: a) M3 muscarinic receptor without any ligand; b) M3 muscarinic receptor docking with tiotropium; c) M3 muscarinic receptor with N-Methylscopolamine [106].

Water molecules: TP3P water is one of the 3 site water models which are very popular for molecular dynamics simulations because of their simplicity and computational efficiency [108], and it refers to the 3 -point model which is re-parameterized to improve

the energy and density for liquid water, that is why it has been chosen as the water model for the simulations in this thesis.

Lipids: In this study we use POPC lipid and the parameters were taken from references [109-111].

All proteins arranged with the lipid bilayer and the water molecules. After equilibration and minimization, molecular dynamic simulation was performed.

2.3.4 Simulations of the M3 muscarinic acetylcholine receptor

In order to understand the structural features of the M3 receptor three different molecular dynamic was performed with the receptor embedded in the lipid bilayer were carried out using GROMACS package 4.6 package. Specifically, trajectories of the M3 receptor embedded in a bilayer of palmitoyl-oleyl phosphatidylcholine (POPC) were run without and with the antagonists N-Methylscopolamine and tiotropium, respectively. The POPC bilayer was considered in this study because it has been widely used in MD simulations of lipid bilayers and its force field parameters have been carefully calibrated and also because they are found in liquid-crystalline phase at temperature condition (300K).

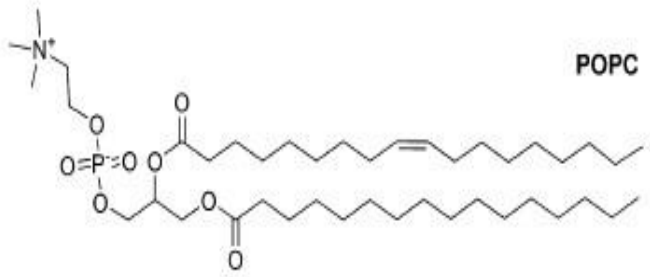

Figure (2.1): Lipid structures used in the Molecular Dynamics Simulations.

Chapter 3: Results and Discussion

3. 0 Overview of the modeling carried out in this work

In the present study we carried out a homology modeling study of the M3 muscarinic receptor using the crystal structure of the M2 muscarinic receptor as template [112] (entry 3UON of the Protein Data Bank), by means of the MOE software. For this purpose we carried out the alignment of the two sequences in order to identify the helical and loop segments of the protein. Prior to be used as a template in homology modeling process, the crystal structure of M2 had to be prepared. The raw structure contains an insertion of a T4-Lysozyme (T4L) in the third intracellular loop. The main purpose of insertion of T4L is to facilitate the growth of diffraction crystals during crystallization purposes [33, 112]. Thus before proceeding to build a homology model of a target protein, the T4L had to be removed.

After template preparation, an alignment of the template and target sequences was done. In accordance with the alignment results, a rough model of the M3 receptor was built using MOE software. Through visualization and MOE utilities, the constructed model was checked for close contacts and subsequently the backbone dihedral angles were projected on the Ramachandran plot.

Once structure validation was completed, two docking calculation were performed to the rough model of M3 muscarinic receptor: docking of antagonists tiotropium and N-Methylscopolamine (see sections 1.4.1 and 1.4.2). Both ligands separately were docked into the binding pocket of the M3 receptor using the MOE induced fit protocol and the GOLD placement algorithms. The results obtained are consistent with those previously reported by Martinez *et al.* for N-Methylscopolamine and Krus *et al.* for tiotropium [113, 114] (see figure 3.1 and figure 3.2). Henceforth, two protein-ligand complexes of M3 muscarinic receptor were available for refinement with molecular dynamic simulations. In addition, as for the main objective of this study, a rough model of the protein without ligand was also put into refinement processes for comparison purposes.

As mentioned above, refinement of the structures was carried out using molecular dynamics (MD) simulations. For this purpose, three separately MD simulations of the models embedded in a lipid bilayer of POPC were performed. Among others, the analysis of the trajectories permitted to identify different conformations adopted by the loops and the effect of the ligand on the protein structure. Finally, in order to understand the

accuracy of the models were compared with the crystal structure of M3 available from the protein data bank (entry 4DAJ of the protein data bank).

3.1. Sequence alignment and homology modeling

The sequences of the human M2 and M3 muscarinic receptor were retrieved from the UNIPROT website [2] and the sequence alignment was done using the program *CLUSTALW* [3] (Table 3.1). The alignment parameters included: no gaps on the transmembrane helices, a correct alignment of the conserved amino acids of the GPCR family according to the figure(3.1) and also, taking into account the range of lengths of inter-helical loops observed over the whole receptor family as shown in table(3.1) [36]. In addition, the sequence of M3 muscarinic receptor used was modified at the third intracellular loop. Both M2 and M3 and other subtypes of muscarinic receptors have a long i3, whose portion can be deleted without interfering with the general functions of the receptor. Thus, based on the number of i3 residues removed in the M2 muscarinic crystal structure, a portion of i3 was excluded and removed from the alignment and subsequent homology modeling.

Table (3.1): Range of the lengths of inter-helical loops over the whole receptor family [32].Intra/extra

	E	**I**	**E**	**I**	**E**	**I**	**E**	**I**
Region	N-TER	I-II	I-III	III-IV	IV-V	V-VI	VI-VII	C-TER
Min size	6	5	13	10	12	12	8	12
Max size	394	11	22	18	43	420	20	162

[2] (*http://ww[2]w.uniprot.org/)*
[3] *http://www.genome.jp/tools/clustalw/*

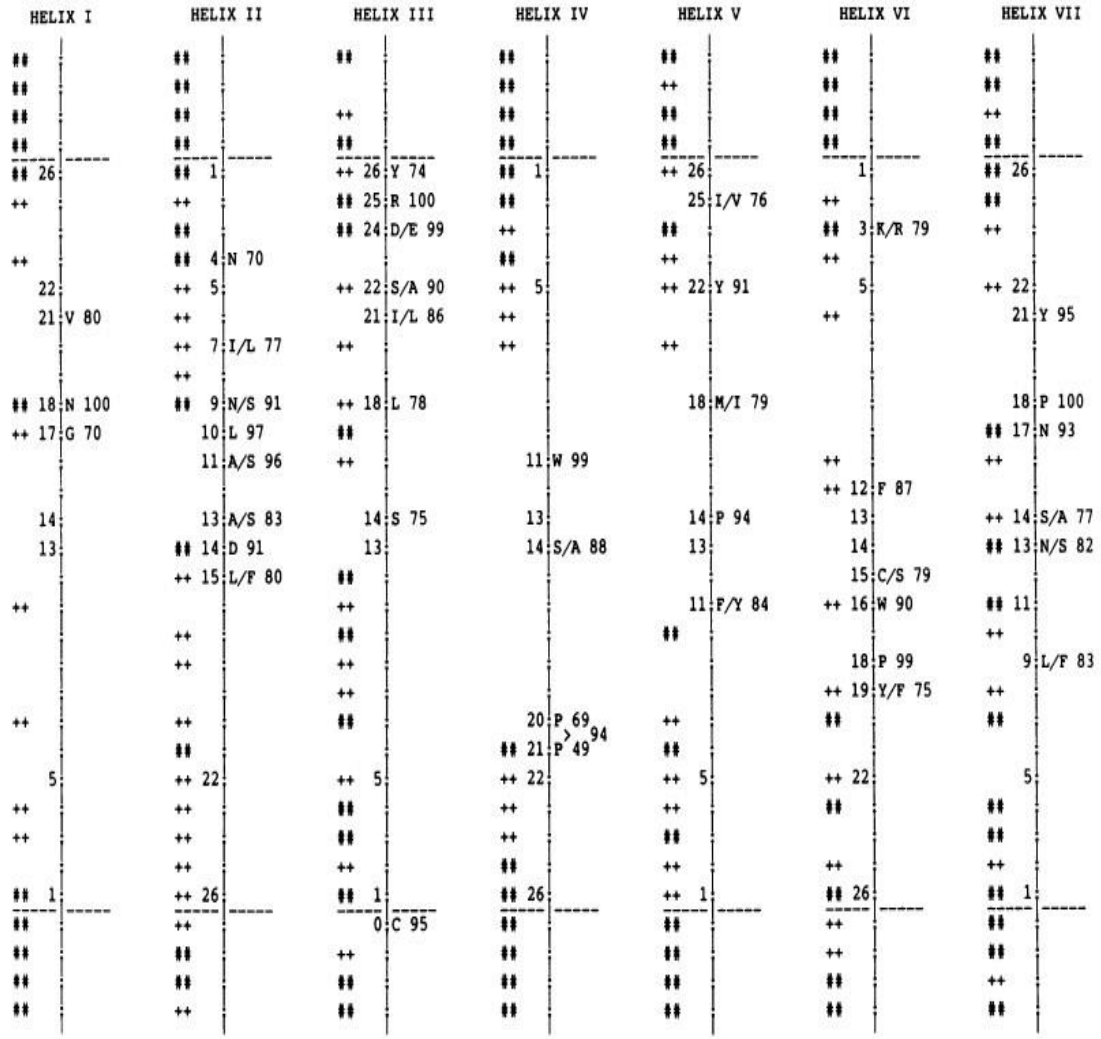

Figure (3.1). Residues that are characteristic for each helix and the distribution of polar residues. Positions in each helix are numbered on the left, upwards for segments T, HI, V, VII and downwards for segments TI, IV and VI; the intracellular surface of the membrane is at the top of the figure. The symbols on the left of the position numbers indicate that a site is occupied by a polar residue in a few sequences (+ +) or in > 10% of the sequences (# #). No symbol on the left indicates that there is never a polar residue at the site. ('Polar' residues include Asp, Asn, Glu, Gln, His,Arg, Lys; all others are regarded as able to face the lipid.) The highly conserved residues in each helix are labelled to the right. The percentage occurrence of the labelled residue (or one of the labelled pair) in 105 unique sequences is shown to the right of the label [36].

In the pairwise sequence alignment, M2 and M3 muscarinic receptors were observed to exhibits an average of 77% sequence homology on the transmembrane segments (as shown in Table 3.2). Furthermore, best score of sequence identity is found in helix three and the lowest in helix 1 (as can be seen in table 3.3).

Table (3.2): Sequence alignment of M2 and M3

```
Sp|P08172|ACM2_HUMAN
Sp|P20309|ACM3_HUMAN

-----------------------------------------------MNNST
MTLHNNSTTSPLFPNISSSWIHSPSDAGLPPGTVTHFGSYNVSRAAGNFS

NSSNNSLALTSPYKTFEVVFIVLVAGSLSLVTIIGNILVMVSIKVNRHLQ
SPDGTTDDPLGGHTVWQVVFIAFLTGILALVTIIGNILVIVSFKVNKQLK
.....:    :..::****.:::* *:**********:**:***::*:

TVNNYFLFSLACADLIIGVFSMNLYTLYTVIGYWPLGPVVCDLWLALDYV
TVNNYFLLSLACADLIIGVISMNLFTTYIIMNRWALGNLACDLWLAIDYV
*******:***********:****:** :. *.** :.*******:***

VSNASVMNLLIISFDRYFCVTKPLTYPVKRTTKMAGMMIAAAWVLSFILW
ASNASVMNLLVISFDRYFSITRPLTYRAKRTTKRAGVMIGLAWVISFVLW
.*********:*******.:*:****.***** **:**. ***:**:**

APAILFWQFIVGVRTVEDGECYIQFFSNAAVTFGTAIAAFYLPVIIMTVL
APAILFWQYFVGKRTVPPGECFIQFLSEPTITFGTAIAAFYMPVTIMTIL
********::** *** ***:***:*:.::**********:** ***:*

YWHISRASKSRIPPPSREKKVTRTILAILLAFIITWAPYNVMVLINTFCA
YWRIYKETEKRTMSLVKEKKAAQTLSAILLAFIITWTPYNIMVLVNTFCD
**:* : ::.*  .  :***.::*: **********:***:***:****

PCIPNTVWTIGYWLCYINSTINPACYALCNATFKKTFKHLLMCHYKNIGA
SCIPKTFWNLGYWLCYINSTVNPVCYALCNKTFRTTFKMLLLCQCDKKKR
.***:*.*.:**********:**.****** **:.*** **:*: .:

TR-------------------
RKQQYQQRQSVIFHKRAPEQAL
  .
```

Table (3.3): Score of identity residues in helixes

```
H1M2            VVFIVLVAGSLSLVTIIGNILVM-
H1M3            VVFIAFLTGILALVTIIGNILVIV
****.:::* *:**********:
Helix1 Aligned. Score: 69.5652
H2M2            YFLFSLACADLIIGVFSMNLY
H2M3            YFLLSLACADLIIGVISMNLF
                ***:**********:****:
Helix2 Aligned. Score: 85.7143
H3M2            LWLALDYVVSNASVMNLLIISF
H3M3            LWLAIDYVASNASVMNLLVISF
                ****:***.*********:***
Helix3 Aligned. Score: 86.3636
H4M2            AGMMIAAAWVLSFILWAPAILFW
H4M3            AGVMIGLAWVISFVLWAPAILFW
                **:**. ***:**:*********
Helix4 Aligned. Score: 78.2609
H5M2            AVTFGTAIAAFYLPVIIMTVLYW
H5M3            TITFGTAIAAFYMPVTIMTILYW
                ::**********:** ***:***
Helix5 Aligned. Score: 78.2609
H6M2            ILAILLAFIITWAPYNVMVLI
H6M3            LSAILLAFIITWTPYNIMVLV
                : **********:***:***:
Helix6 Aligned. Score: 76.1905
H7M2            IGYWLCYINSTINPACYALC
H7M3            LGYWLCYINSTVNPVCYALC
                :**********:**.*****
Helix7 Aligned. Score: 85
```

Furthermore, during alignment of the two sequences the following considerations were taken into account in order to build the model:

I. Starting and finishing points for each of the 7 helixes
II. Check that conserved residues align together
III. Check the position of two cysteine residues of the disulfide bridge
IV. Alignment of big loops together (small loops are not important as big loops) Table 3.4 shows a detailed comparison of the conserved residues and the different motifs deduced from the sequence alignment.

Extracellular loops

The resulting M3 muscarinic receptor model has similar length and loop morphology as that of the template M2 muscarinic receptor. Accordingly, the disulfide bridges observed in M2 muscarinic receptor were also conserved in M3 muscarinic receptor. In the target receptor these bridges were observed to be between Cys140 of the N-terminus of helix 3 and Cys220 of the second extracellular loop, and between Cys516 and Cys519 of the third extracellular loop including the directly neighbored amino acids were as depicted in the M2 muscarinic acetylcholine receptor (see figure (3.2).

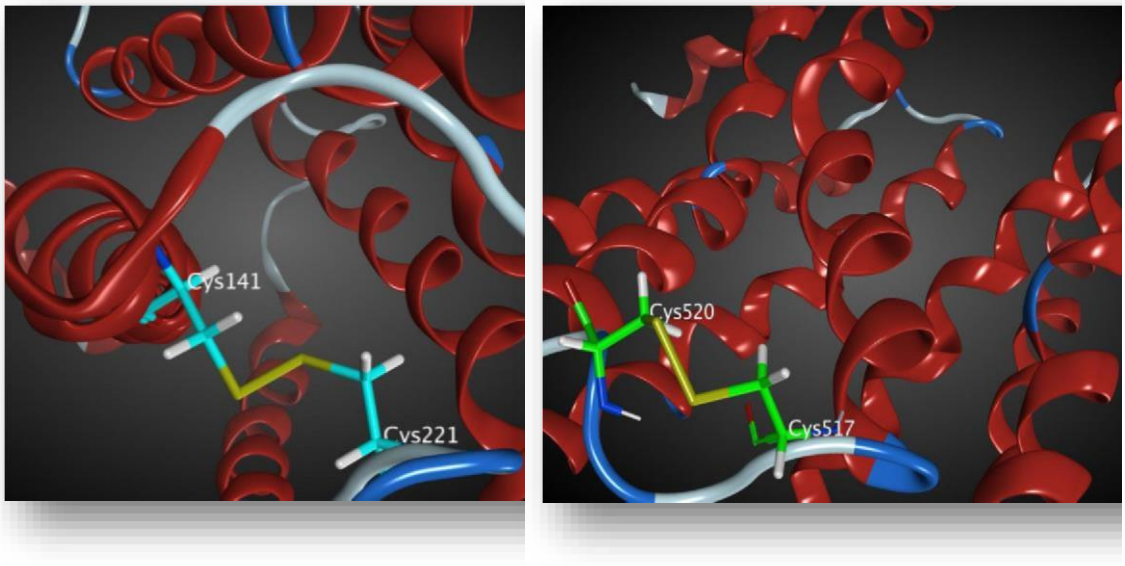

Figure (3.2): The two disulfide bridges in the structure of M3 muscarinic receptor between Cys140-Cys220 and also Cys516-Cys 519(numbering of residues appear in all the figures shifted one residue)

Table (3.4): Result position of Conserve Residue of the study

```
ACM2_HUMAN
ACM3_HUMAN

N-terminus
TFE
VWQ

Helix 1 (H1)
VVFIVLVAGSLSLVTIIGNILVMVSIKV
VVFIAFLTGILALVTIIGNILVIVSFKV

Intracellular loop 1 (ICL1)
NRHLQT
NKQLKT

Helix 2
VNNYFEFSLACADEIIGVFSMNLYTLYTV
VNNYFELSLACADEIIGVISMNLFTTYII

Extra cellular loop 1 (ECL1)
IGYWPLG
MNRWALG

Helix 3 (H3)
PVVCDLWLALDYVVSNASVMNLLIISFDRYFCVT
NLACDLWLAIDYVASNASVMNLLVISFDRYFSIT

Intracellular loop 2(ICL2)
KPLTYPVKRT
RPLTYRAKRT

Helix 4 (H4)
TKMAGMMIAAAWVLSFILWAPAILFWQFIV
TKRAGVMIGLAWVISFVLWAPAILFWQYFV

Extra cellular loop 2 (ECL2)
GVRTVEDGECYIQFFSN
GKRTVPPGECFIQFLSE

Helix 5 (H5)
AAVTFGTAIAAFYLPVIIMTVLYWHISRAS
PTITFGTAIAAFYMPVTIMTILYWRIYKET

Intracellular loop 3(ICL3)
KSRIPPPSREK
EKRTMSLVKEK

Helix 6 (H6)
KVTRTILAILLAFIITWAPYNVMVLINTF
KAAQTLSAILLAFIITWTPYNIMVLVNTF

Extra cellular loop 3 (ECL3)
CAPCIP
CDSCIP

Helix 7 (H7)
NTVWTIGYWLCYINSTINPACYALCNATFKKTFKHL
KTFWNLGYWLCYINSTVNPVCYALCNKTFRTTFKML

C-Terminus
LM
LL
```

Intracellular loops

As observed in the extracellular loops, the intracellular loops of the constructed M3 muscarinic model were similar to those of the template M2 muscarinic receptor. As seen in previous studies [115], a similarity in length and predicted secondary structure was observed between M2 and M3 muscarinic receptors. Accordingly, the coordinates of M2 muscarinic receptor were accepted for the M3 model.

N-terminus/ C-terminus

The secondary structure of the N-terminus and C- terminus of target M3 muscarinic receptor were also similar to the template M2 muscarinic receptor.

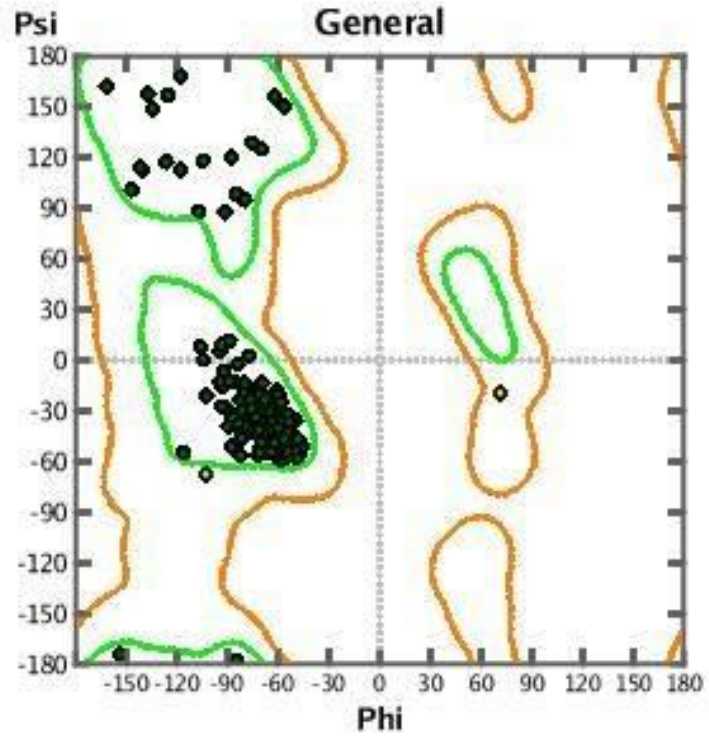

Figure (3.3): Ramachandran map for human M3 muscarinic receptor showing that 100% of the observed dihedral angles are clustered in the sterically allowed regions.

Overall Structure validation

Once a rough homology model of the M3 receptor was constructed using the constructed MOE, the software was used to validate the model. The validation process aims to check the stereochemically quality of all protein chains. This is done by visualizing the bonds or clashes in between atoms in the model and by computing the values of the backbone torsional angles and plotting them in a Ramachandran map to show the distribution of angles observed in a single structure. Figure (3.3) shows that all the angles in the

constructed M3 muscarinic receptor model are clustered into the allowed stereochemical regions of the map.

3.2. Analysis of the orthosteric binding site

The orthosteric binding site is the classical binding site where the muscarinic antagonists tiotropium or N-Methylscopolamine bind. Previous docking studies of NMethylscopolamine bound to the M3 receptors [114] and tiotropium docked to a model of M3 [55] suggested different residues involved in recognition (Table 3.5). These residues were used to guide the docking of the ligands in the present work.

Table (3.5): Residues involved in the antagonists binding to M3 muscarinic receptor

Antagonist	**Binding pockets residue**
Tiotropium	Asp147,Tyr148,Trp199,Thr231,Phe239,Tyr506,Asn507,Tyr529, Cys532,Tyr533
NMS	Asp147,Ser151,Asn152,Phe221(ECL2),Ile222(ECL2),Thr234,Ala235, Ala238, Trp503, Asn507, Val510, Leu511, Cys532 and Tyr533.

Several induced fit molecular docking calculations of tiotropium and N-methyl scopolamine to the constructed model of M3 muscarinic receptor were carried out using MOE software and GOLD placement algorithm. The resulted poses were rank ordered by binding/docking score and for each of the ligands, the binding pose with the best binding score were selected. Figures 3.4 and 3.5 show the residues involved in the binding pocket of the M3 muscarinic receptor modeled of tiotropium and N-methyl scopolamine respectively.

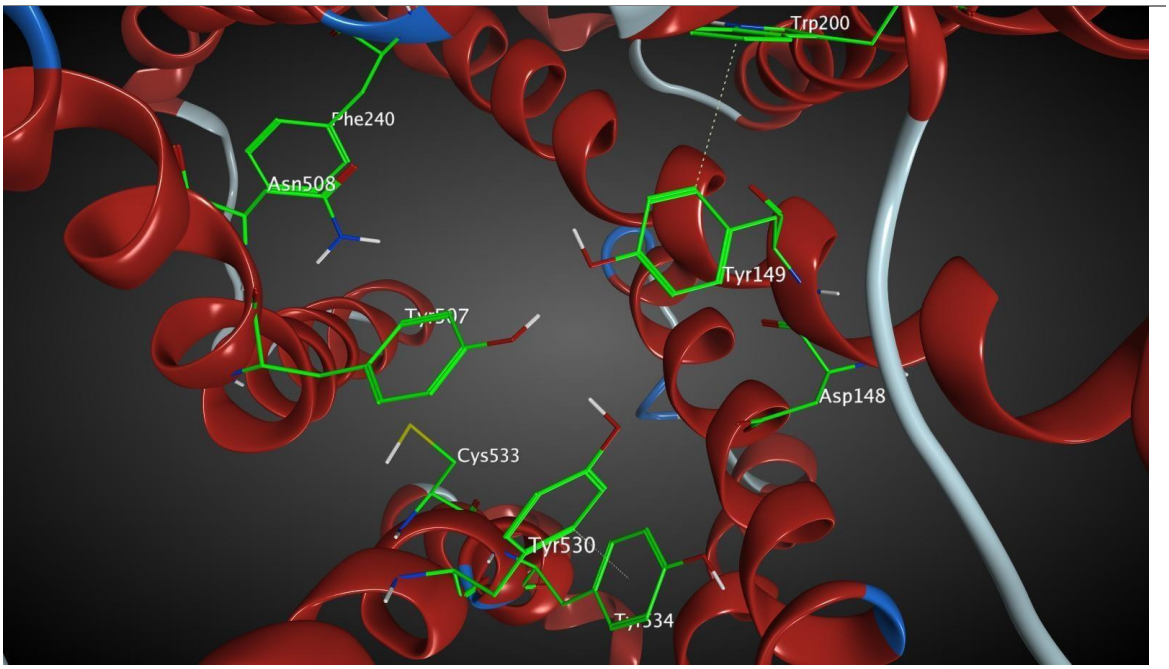

Figure (3.4): Binding pocket of tiotropium. Residues directly involved in binding the ligand are: Asp147,Tyr148,Trp199,Thr231,Phe239,Tyr506,Asn507,Tyr529, Cys532,Tyr533(numbering of residues appear in all the figures shifted one residue)

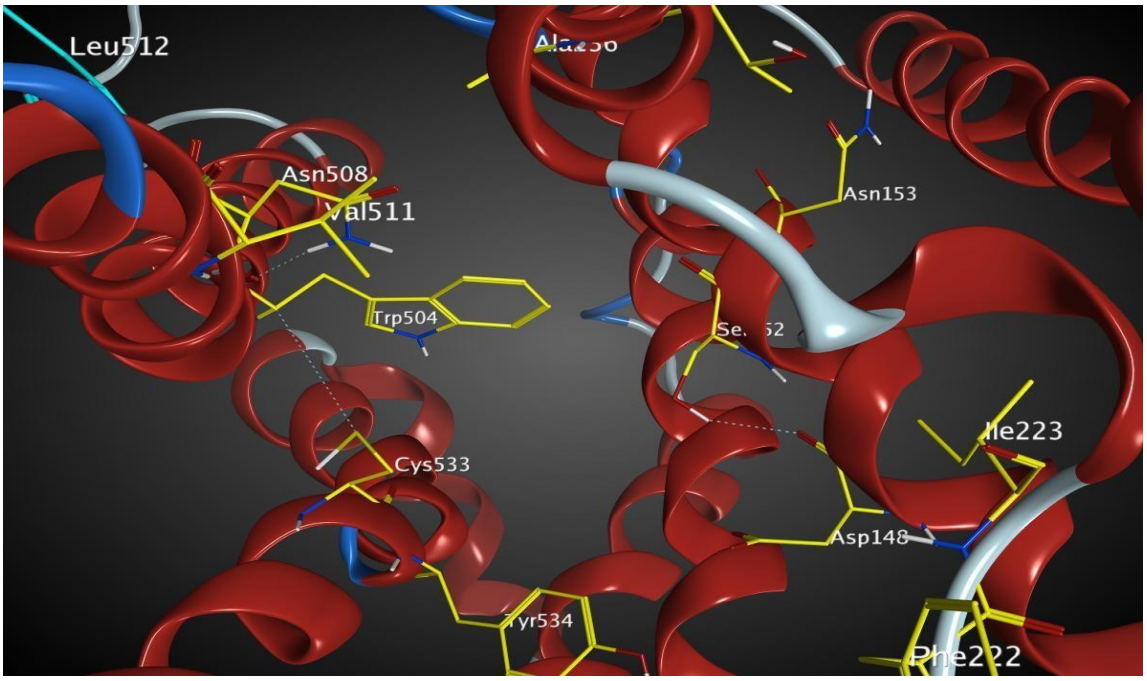

Figure (3.5): Bonding pocket of N-Methylscopolamine: Residues directly involved in binding the ligand are : Asp147,Ser151,Asn152,Phe221(ECL2),Ile222(ECL2),Thr234,Ala235, Ala238, Trp503, Asn507, Val510, Leu511, Cys532 and Tyr533. (Numbering of residues appear in all the figures shifted one residue)

3.3: Analysis of interactions

According to Kruse *et al.* [49], in the M3 muscarinic receptor similarly to M2 muscarinic receptor, the ligand tiotropium is deeply buried within the 7TM receptor core and is covered by a lid comprising three conserved tyrosines (Tyr148, Tyr506 and Tyr529). The ligand is almost completely occluded from solvent and engages in extensive hydrophobic contacts with the receptor. A pair of hydrogen bonds are formed fromAsn507 to the ligand carbonyl and hydroxyl, while Asp147 interacts with the amine group of the ligand. Figure 3.6 (a and b) shows the protein-ligand interactions between tiotropium and the M3 muscarinic receptor as depicted by the best binding score and pose resulted from the molecular docking calculations.

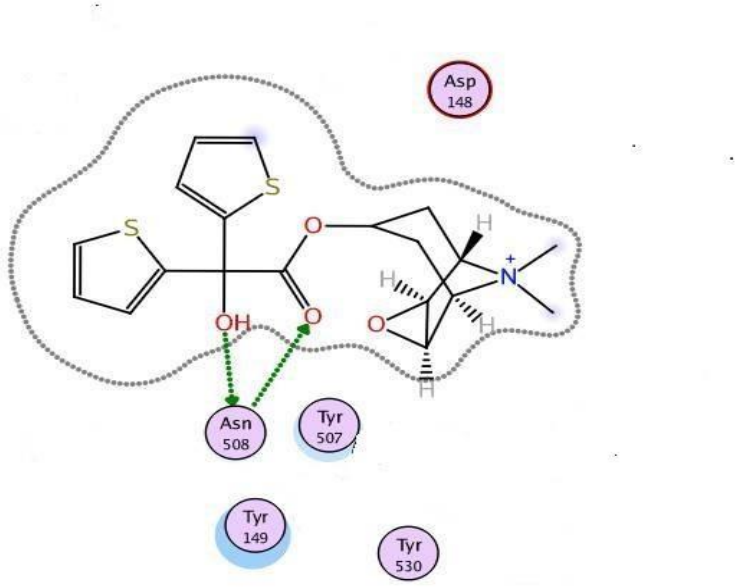

Figure 3.6a: a 2D representation of the interactions between ligand tiotropium and residues in the antagonist binding pocket of M3 muscarinic receptors. . (Numbering of residues appear in all the figures shifted one residue)

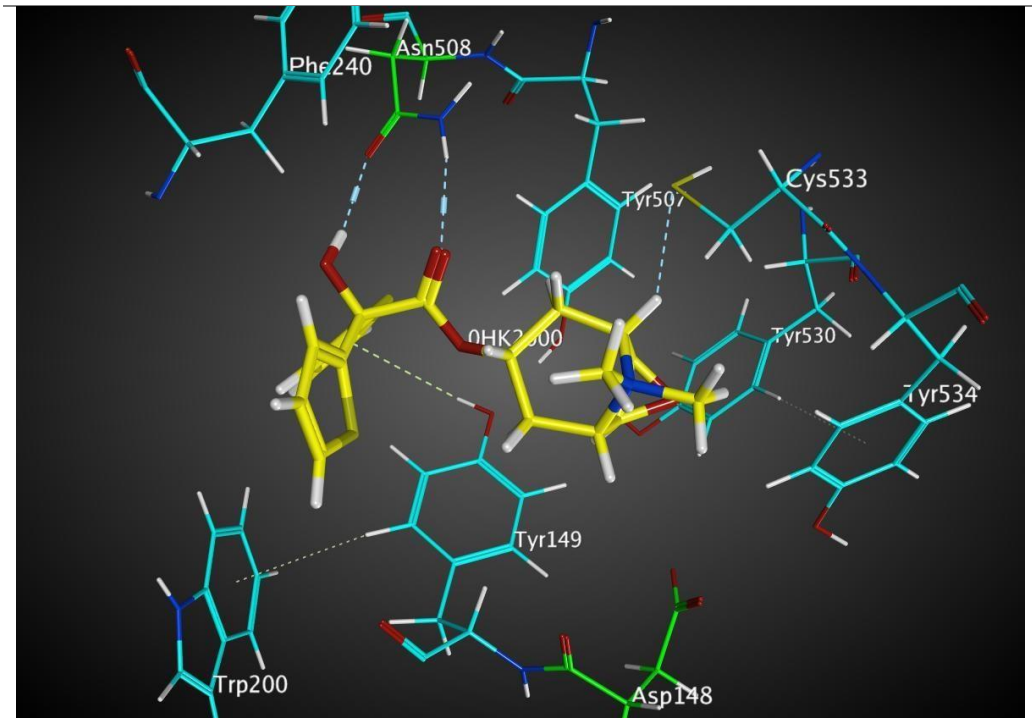

Figure 3.6b: a 3D representation of the interaction between ligand tiotropium and residues in the antagonist binding pocket of M3 muscarinic receptors. . (Numbering of residues appear in all the figures shifted one residue)

As shown in figure 3.6, the ligand is surrounded by Tyr 148, Tyr506, Tyr529, Asn507 and Asp147. Among the interacting residues, Asn507 and Asp147 are notably the most important ones. The former forms a hydrogen bond with the carbonyl and hydroxyl moieties, and the latter forms an interaction with the amine group, with distance of 4.7 Å. This distance is long for a hydrogen bond interaction, although it could be mediated by a water molecule.

In case of N-Methylscopolamine, several binding studies have identified Asp147 to be most important in N-Methylscopolamine binding. This residue is known to interact with the ligand quaternary nitrogen. Putatively, Asn507 involved in a polar interaction with the ligand, and the homologous hydrophobic residues implicated in the binding of N-Methylscopolamine at the M3 muscarinic receptor.

Figure 3.7 shows the protein-ligand interactions between N-Methylscopolamine and the M3 muscarinic receptor as depicted by the best binding score and pose resulted from the molecular docking calculations.

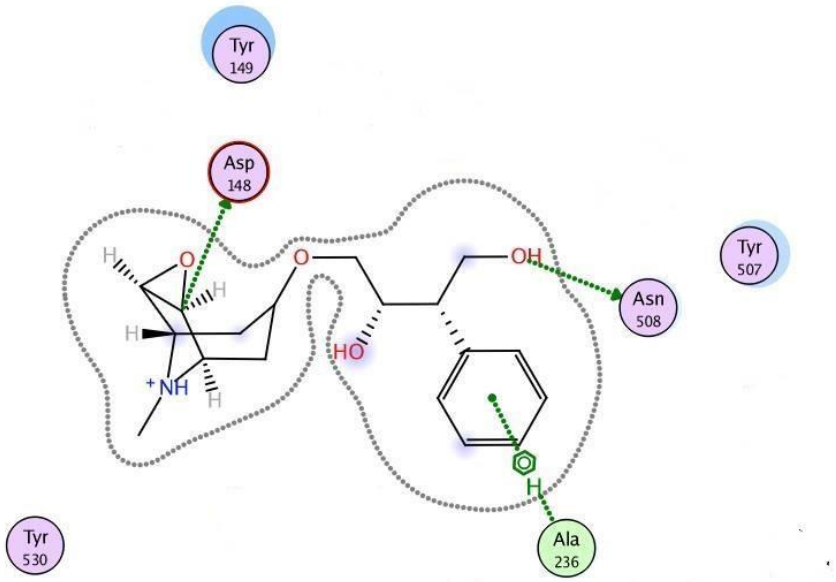

Figure 3.7a: a 2D representation of the interaction between ligand N-Methylscopolamine and residues in the antagonist binding pocket of M3 muscarinic receptors. **.** (Numbering of residues appear in all the figures shifted one residue)

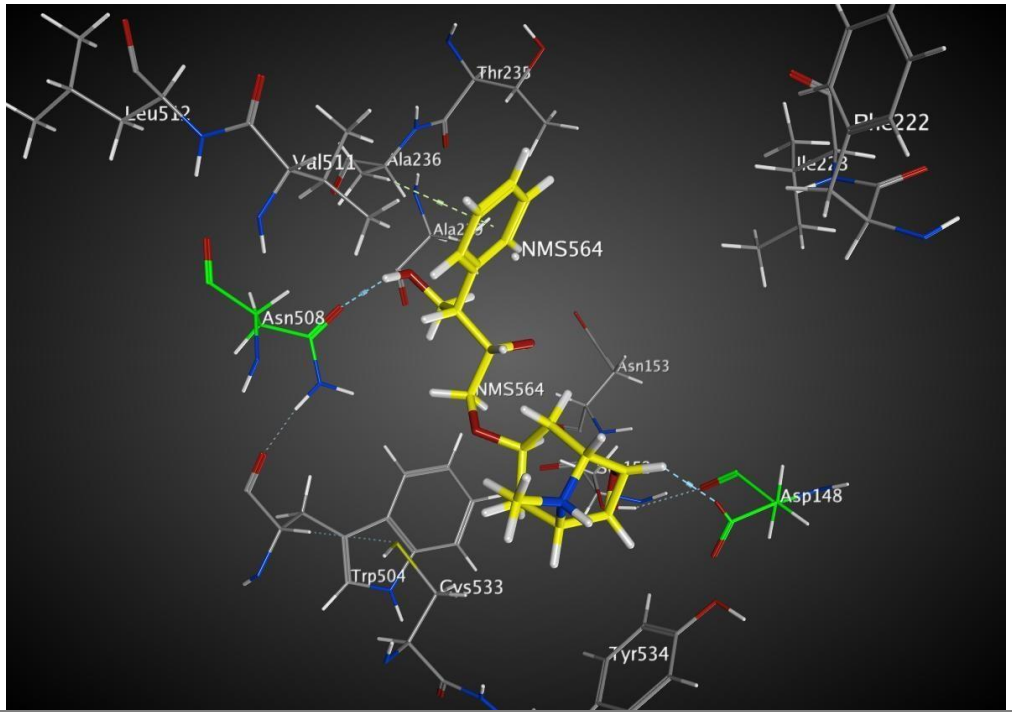

Figure 3.7b: a 3D representation of the interaction between ligand N-Methylscopolamine and residues in the antagonist binding pocket of M3 muscarinic receptors. . (Numbering of residues appear in all the figures shifted one residue)

3.4. Structural analysis of the refined M3 muscarinic receptor

MD simulations provides detailed information on the fluctuations and conformational changes of proteins and nucleic acids. These methods are now routinely used to investigate the structure and dynamics of biological molecules and their complexes, and investigate the influence of ligand inside the binding pocket of the receptor. Three molecular dynamic stimulation were computed using the GROMACS 4.6 package [111]. One molecular dynamics simulation with the receptor M3 muscarinic receptor without any ligand, another one molecular dynamic simulation of tiotropium inside the binding pocket of M3 muscarinic receptor and the final simulation was the ligand N-Methylscopolamine inside the binding pocket of the M3 muscarinic receptor, in all simulations, protein only or protein ligand(s) complex) were embedded in POPC lipid bilayer. POPC lipid bilayer, was selected since the force field parameters of this lipid are well known.

3.4.1 Structure equilibration

Equilibration of these systems require long simulation times. The root-mean-square deviation (rmsd) of the backbone atoms of the protein can be used to monitor the evolution of the system. The time evolution of the root mean square deviation in the different simulations performed in the present work, are illustrated in figure (3.8). As can be seen for the systems with tiotropium and N-Methylscopolamine, equilibration appears after 50 ns, whereas in the simulation without ligand equilibration requires longer times of about 350 ns. However, it should be taken into account that much shorter times can be observed if only the helical section of the receptors are considered.

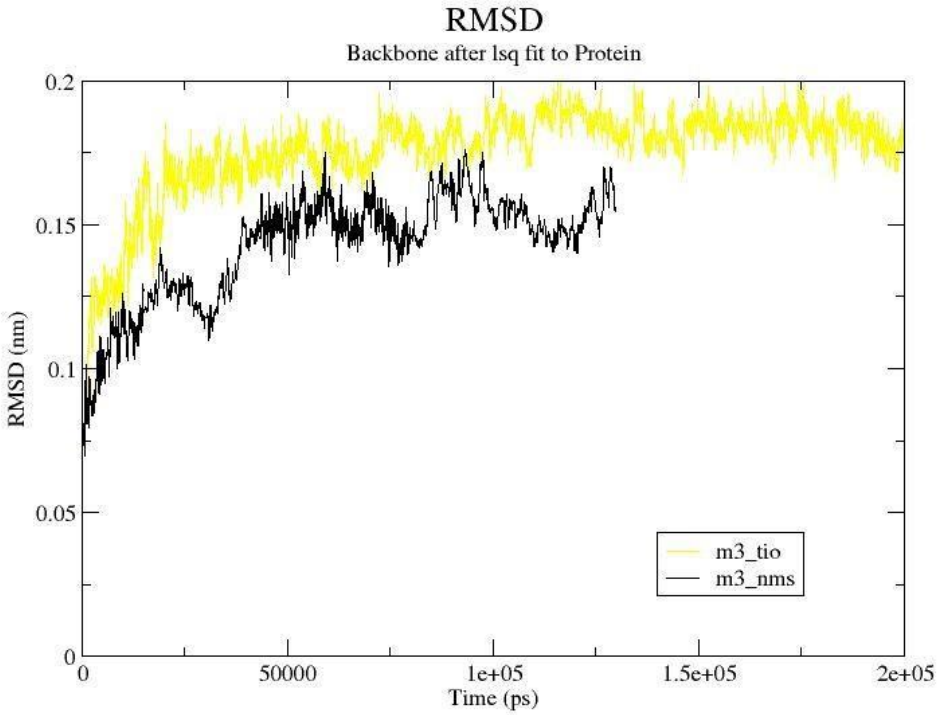
RMSD
Backbone after lsq fit to Protein
RMSD (nm)
0.2
0.15
0.1
0.05
0
0
50000
1e+05
1.5e+05
2e+05
Time (ps)
m3_tio
m3_nms

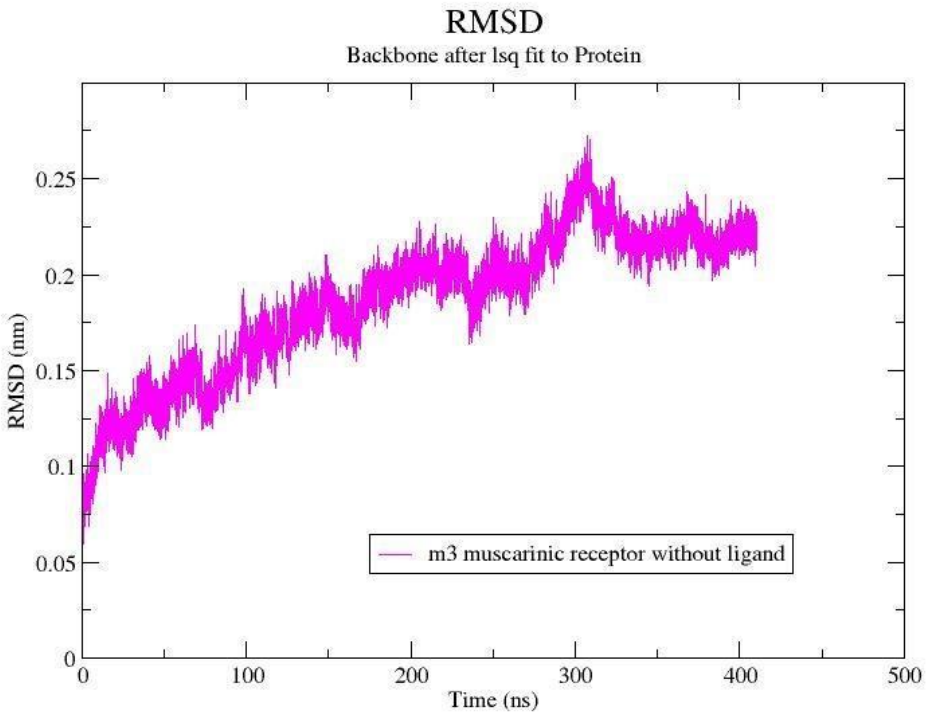
RMSD
Backbone after lsq fit to Protein
RMSD (nm)
0.25
0.2
0.15
0.1
0.05
0
0
100
200
300
400
500
Time (ns)
m3 muscarinic receptor without ligand

Figure (3.8): Time evolution of root mean square deviation (rmsd) of the backbone atoms of M3 receptors. a) Evaluation of M3 with N-Methylscopolamine and tiotropium docked inside; b) M3 structure without ligand

Analysis of these plots suggest that for proper analysis, only the stable part of the time graph should be considered.

Table (3.6): Different simulations performed.

Structures	***MD Production Times***
M3 muscarinic receptor without any ligand	110ns
M3 muscarinic with tiotropium bound to its orthosteric binding pocket.	243ns
M3 muscarinic with N-Methylscopolamine bound to its orthosteric binding pocket.	100ns

3.1.2 Rmsf per residue

Rmsf per residue is a suitable tool to describe comparison of deviation among helices and intracellular/extracellular loops of M3 receptor that has been modeled.

Rmsf values per residue highlighted less mobility in the backbone region of the M3 receptor than in the connecting loops (as shown in Figure 3.9). The largest deviations correspond mainly to the second and third intra-cellular loops of the protein (deviations above 1nm) whereas the smallest ones are shown in the transmembrane region of the protein. That fact may be related functional-wise to the assumption that receptor G protein/coupling occurs through intracellular loops in all of the muscarinic acetylcholine receptors as previously anticipated [116]. It should also be factored that, these largest deviations were observed in loops that are long.

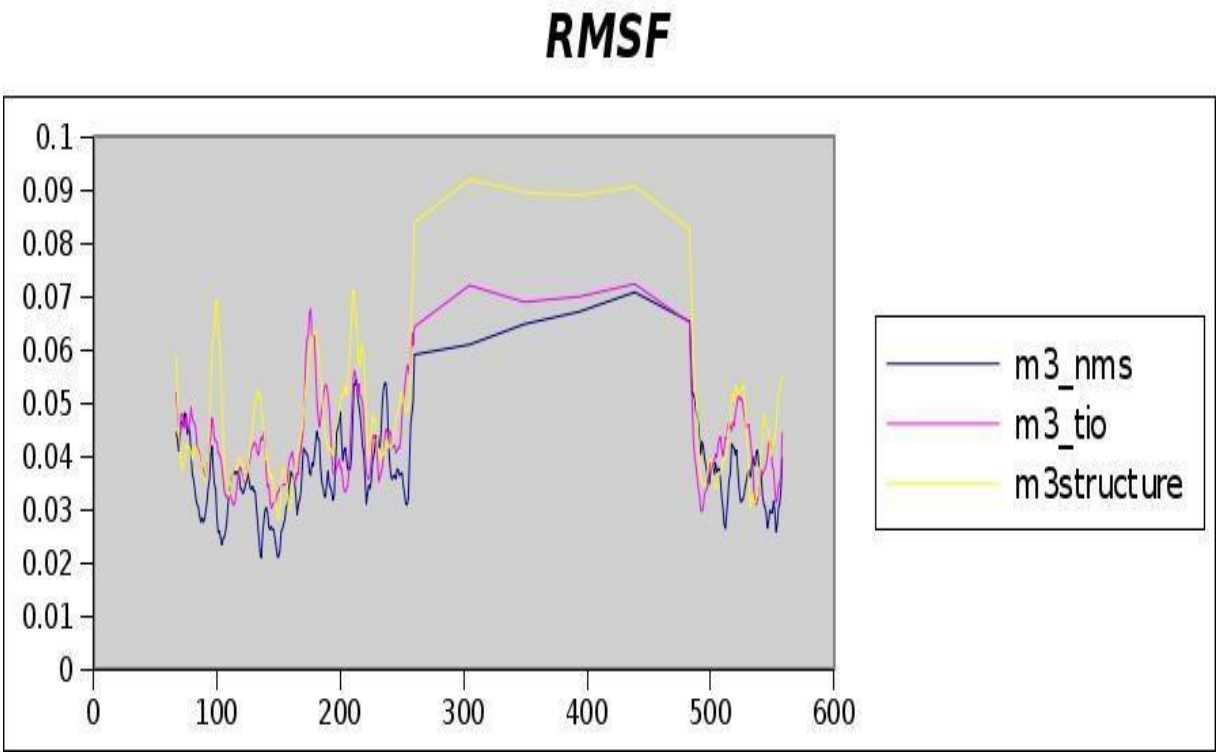

Figure (3.9): Average root mean square fluctuation (rmsf) of the backbone atoms of each residue in three MD simulations performed.

Because residue 262-481 of all structures has been removed, this part can be seen as flat part in the graph. Loops of the M3 muscarinic receptor without any ligand were observed to have more fluctuations in comparison to M3 muscarinic receptor with ligand tiotropium or NMS (complexes).

In drawing comparison between the average structures obtained in three simulations, structural deviations are not very large (Figure 3.10) and Table (3.7).The superposition of α carbon of the average structure of the refined (after MD simulations) M3 muscarinic receptor-ligand complex models, showed similarity to each other and to the crystal structure of M3 muscarinic receptor complexes with tiotropium. In contrast, a refined model of M3 muscarinic receptor without ligand and more structural deviations. Major differences are observed in the third intracellular loop and third extracellular loop. In fact, it is also where the M3 structure is more flexible, and have more movement after molecular dynamic simulation.

Table (3.7): Average RMSD of α carbon of the structure after superposition of three model together

Structures	RMSD(Å)
M3 muscarinic receptor: m3_tio	2.36
M3 muscarinic receptor: m3_nms	2.16
M3_tio:m3_nms	2.21

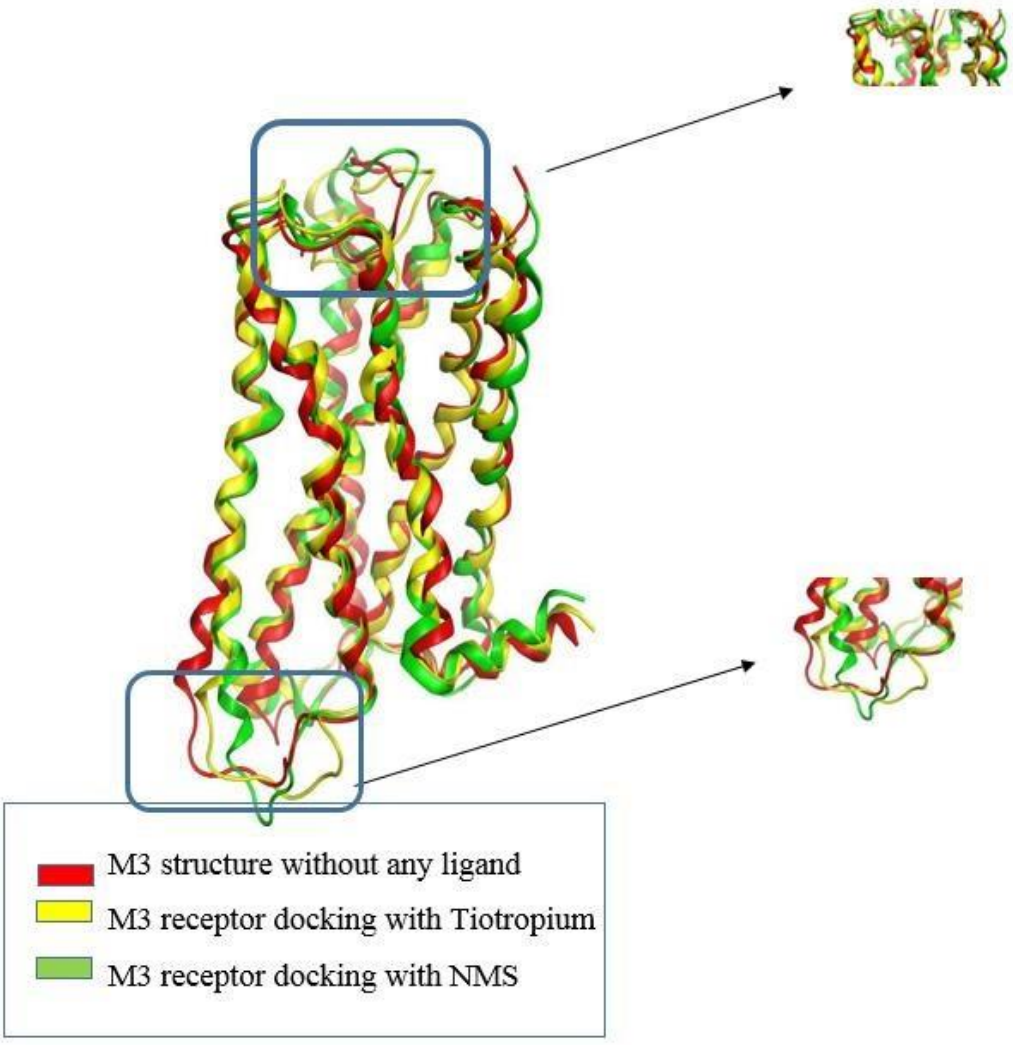

Figure (3.10): α carbon superposition of average three models of M3 constructed. As a blow up the third intracellular loop shows the largest deviations between the three models.

3.1.4. Comparison of constructed models with crystal structure of M3 muscarinic receptor

The most critical assessment of the quality of the models regards direct comparison of the refined models (average structures obtained from MD simulations) with the crystal Structure of M3 muscarinic receptor with tiotropium bound to it (entry 4DAJ of the protein data bank). The main objective of this comparison was to measure the accuracy of the methodology used in this study to predict and construct useful GPCR models. Accordingly, three refined models were superimposed with the crystal structure. Overall the models do not show much differences with the crystal structure (see Figure 3.11). In fact, superimposition of the Cα of these structures shows that deviations are not very large. The closest models are those that included ligand with deviations between 1.7 and 2.0 Å, whereas the model produced without ligand deviations are much longer (2.5 Å).

Structure	shape	RMSD (Å)
M3muscurinic receptor	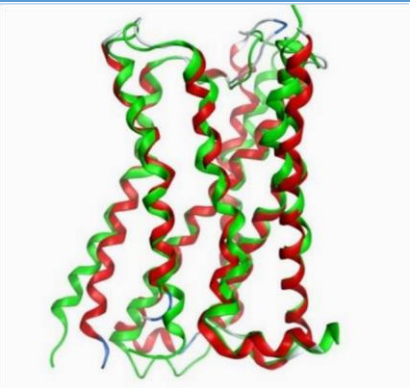	2.5
M3_tio	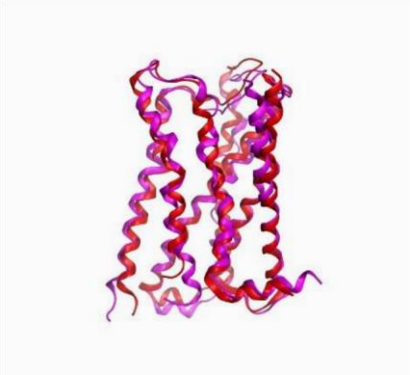	2.1

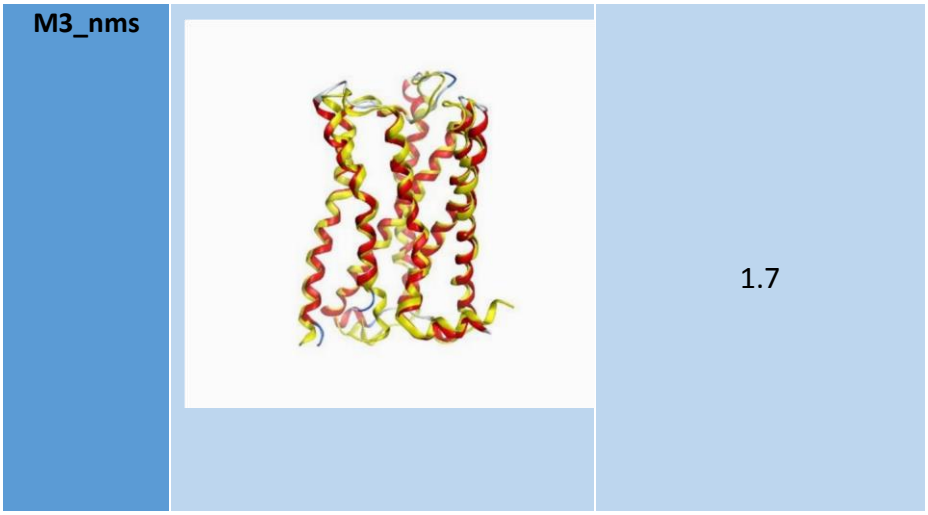

Figure 3.11: Superposition of average refined models and the crystal structure of M3 muscarinic receptor (In all of them crystal M3 muscarinic receptor shows in red color)

A closer inspection of the superimposition of the models and the crystal structure reveal some differences. An important issue in the modeling is the accuracy of the predicted helices. Table (3.8) shows a comparison of the features of the models with the crystal structure regarding the beginning and the ending of the helices.

Table (3-8): comparison of residues in transmembrane helixes of homology model and crystal structure of M3 muscarinic receptor

	Model	**Crystal structure**
Transmembrane Helix 1	Trp65-Val 94	Trp65-Val94
Transmembrane Helix 2	Va101-Asn131	Val101-Met130
Transmembrane Helix 3	Asn138-Arg171	Gly137-Arg171
Transmembrane Helix 4	Val186-Val 210	Thr181-Val 210
Transmembrane Helix 5	Pro228-Lys260	Pro228-N/A
Transmembrane Helix 6	Gln490-Cys516	N/A-Cys516
Transmembrane Helix 7	Lys522-Leu558	Lys522-Lys555

Analysis of the Table (3.8) reveals that errors are less than one helix turn in most of the helices, except in TM4 after the second intracellular loop with more than a helix turn difference. The end of TM5 and the beginning of TM6 connected by the third intracellular loop cannot be really compared due to the presence of lysozyme both in the crystal structure of M3 muscarinic receptor and in the template used in the homology modeling (M2 muscarinic receptor). As mentioned in sections 1.2.2 and 3.1, the third intracellular loop is considerably long for all muscarinic receptor subtypes A deletion of portion of this loop bears no consequences to the overall function of the GPCR or the binding of G- protein to the GPCR. Thus, the deletion of part of the intracellular loop (219 residues were deleted during template- target sequence alignment), may have contributed to the one helical turn error.

Comparison of the crystal structures of M2 and M3 reveal that the structures although very similar exhibit a few differences as reviewed recently [109]. Present models capture most of these features. Thus, for example the position of the ligand deeply buried within the transmembrane core is preserved. In agreement with previous models of M3 muscarinic receptor, Asp147 and Asn507 which are two of the highly conserved residue among all biogenic amine receptors, are essential for binding at the M3 muscarinic receptor to antagonists. The results show that arginine which is part of the highly conserved DRY sequence has got an essential functional role in GPCRs. Also ion pair between the ammonium group of acetylcholine and a conserved aspartate residue in the TM3 segment (transmembrane segment of helix 3) (Asp147 in M3) plays a key role in complex stabilization, which also was identified by Gromada and Hughes [55]. This negatively charged residue of TM3 critically interacts with ligands and is indeed a feature common to all GPCRs [30]. Inspection of the side chains of M3 surrounding tiotropium, the model shows that Asp147 and the amine group of the ligand are at a longer distance than expected.

Another feature captured in our model is a difference is the position of residue L225, a phenylalamine (F181) in M2 that creates an extra pocket in M3. However, both structures show a bend -not seen in any other GPCRs crystallized so far- that is stabilized by a hydrogen bond between Q207 (Q163 in M2) side chain and L204 backbone peptide carbonyl. Indeed, mutagenesis of Q207 in M3 impaired both ligand binding and receptor activation that is not captured in our model.

Conclusions

This study present the effect of the presence of a ligand on the modeling of the structure of human M3 receptor. The structure of the M3 muscarinic receptor was constructed by homology modeling using the crystal structure of M2 receptor as template, representing the inactive form of the receptor. The model was refined using molecular dynamics. In the present work we investigated the effect of the ligand on the conformational of protein analysis.

Analysis of the models and their refinement process show that the models constructed capture most of the features of the M3 receptor. Moreover, inclusion of a ligand on the modeling makes the refinement more robust. Analysis of the root-mean-square deviation (rmsd), root-mean-square fluctuations (rmsf) and the equilibration times during the trajectory calculation support this conclusion. Interestingly, experimental evidence supports the idea that ligands stabilize a receptor as shown on the β_2 adrenergic receptor after DTT binds to it analyzed by fluorescence spectroscopy [117]. Similarly, based on conclusions of several studies, binding of ligand can facilitate and improve on protein crystallization processes as shown by the increasing number of structures recently.

References

1. Pedretti, A., et al., *Muscarinic receptors: A comparative analysis of structural features and binding modes through homology modelling and molecular docking.* Chem Biodivers, 2006. **3**(5): p. 481-501.
2. Fredriksson, R. and H.B. Schioth, *The repertoire of G-protein-coupled receptors in fully sequenced genomes.* Molecular Pharmacology, 2005. **67**(5): p. 1414-25.
3. King, N., C.T. Hittinger, and S.B. Carroll, *Evolution of key cell signaling and adhesion protein families predates animal origins.* Science, 2003. **301**(5631): p. 361-3.
4. Cannon, J.G. and M.E. In Wolff, *Cholinergics* Burger's Medicinal Chemistry, 1981: p. 339-360.
5. Filmore, D., *It's a GPCR world.* Modern Drug Discovery (American Chemical Society), 2004: p. 24-28.
6. Hopkins, A.L. and C.R. Groom, *The druggable genome.* Nat Rev Drug Discov, 2002. **1**(9): p. 727-30.
7. Klabunde, T. and G. Hessler, *Drug design strategies for targeting G-proteincoupled receptors.* Chembiochem, 2002. **3**(10): p. 928-44.
8. Overington, J.P., B. Al-Lazikani, and A.L. Hopkins, *How many drug targets are there?* Nat Rev Drug Discov, 2006. **5**(12): p. 993-6.
9. Rama Sastry, B.V. and M.E. In Wolff, *Chirality in Drug Research.* Burger's Medicinal Chemistry, 1981: p. 361 -411.
10. Schoneberg, T., et al., *Mutant G-protein-coupled receptors as a cause of human diseases.* Pharmacol Ther, 2004. **104**(3): p. 173-206.
11. Liu, G., et al., *Leydig-cell tumors caused by an activating mutation of the gene encoding the luteinizing hormone receptor.* N Engl J Med, 1999. **341**(23): p. 1731-6.
12. Xie, J., et al., *Activating Smoothened mutations in sporadic basal-cell carcinoma.* Nature, 1998. **391**(6662): p. 90-2.
13. Rosenthal, W., et al., *Molecular identification of the gene responsible for congenital nephrogenic diabetes insipidus.* Nature, 1992. **359**(6392): p. 233-5.
14. Parma, J., et al., *Somatic mutations in the thyrotropin receptor gene cause hyperfunctioning thyroid adenomas.* Nature, 1993. **365**(6447): p. 649-51.

15. Smits, G., et al., *Ovarian hyperstimulation syndrome due to a mutation in the follicle-stimulating hormone receptor.* N Engl J Med, 2003. **349**(8): p. 760-6.
16. Vasseur, C., et al., *A chorionic gonadotropin-sensitive mutation in the folliclestimulating hormone receptor as a cause of familial gestational spontaneous ovarian hyperstimulation syndrome.* N Engl J Med, 2003. **349**(8): p. 753-9.
17. Robinson, G.C. and J.E. Jan, *Acquired ocular visual impairment in children. 1960-1989.* Am J Dis Child, 1993. **147**(3): p. 325-8.
18. Lubrano-Berthelier, C., et al., *Melanocortin 4 receptor mutations in a large cohort of severely obese adults: prevalence, functional classification, genotypephenotype relationship, and lack of association with binge eating.* J Clin Endocrinol Metab, 2006. **91**(5): p. 1811-8.
19. Bockaert, J., *[G-protein coupled receptors. Nobel Prize 2012 for chemistry to Robert J. Lefkowitz and Brian Kobilka]*. Med Sci (Paris), 2012. **28**(12): p. 1133-7.
20. Shimamura, T., et al., *Crystal structure of squid rhodopsin with intracellularly extended cytoplasmic region.* Journal of Biological Chemistry, 2008. **283**(26): p. 17753-6.
21. Standfuss, J., et al., *Crystal structure of a thermally stable rhodopsin mutant.* J Mol Biol, 2007. **372**(5): p. 1179-88.
22. Warne, T., et al., *Structure of a beta1-adrenergic G-protein-coupled receptor.* Nature, 2008. **454**(7203): p. 486-91.
23. Rasmussen, S.G., et al., *Crystal structure of the human beta2 adrenergic Gprotein-coupled receptor.* Nature, 2007. **450**(7168): p. 383-7.
24. Jaakola, V.P., et al., *The 2.6 angstrom crystal structure of a human A2A adenosine receptor bound to an antagonist.* Science, 2008. **322**(5905): p. 1211-7.
25. Ji, T.H., M. Grossmann, and I. Ji, *G protein-coupled receptors. I. Diversity of receptor-ligand interactions.* Journal of Biological Chemistry, 1998. **273**(28): p. 17299-302.
26. Kolakowski, L.F., Jr., *GCRDb: a G-protein-coupled receptor database.* Receptors Channels, 1994. **2**(1): p. 1-7.
27. Foord, S.M., et al., *International Union of Pharmacology. XLVI. G proteincoupled receptor list.* Pharmacol Rev, 2005. **57**(2): p. 279-88.

28. Joost, P. and A. Methner, *Phylogenetic analysis of 277 human G-proteincoupled receptors as a tool for the prediction of orphan receptor ligands.* Genome Biol, 2002. **3**(11): p. RESEARCH0063.
29. Bjarnadottir, T.K., et al., *Comprehensive repertoire and phylogenetic analysis of the G protein-coupled receptors in human and mouse.* Genomics, 2006. **88**(3): p. 263-73.
30. Hulme, E.C., et al., *The role of charge interactions in muscarinic agonist binding, and receptor-response coupling.* Life Sciences, 1995. **56**(11-12): p. 891-8.
31. Curtis, C.A., et al., *Propylbenzilylcholine mustard labels an acidic residue in transmembrane helix 3 of the muscarinic receptor.* Journal of Biological Chemistry, 1989. **264**(1): p. 489-95.
32. Palczewski, K., et al., *Crystal structure of rhodopsin: A G protein-coupled receptor.* Science, 2000. **289**(5480): p. 739-45.
33. Cherezov, V., et al., *High-resolution crystal structure of an engineered human beta2-adrenergic G protein-coupled receptor.* Science, 2007. **318**(5854): p. 1258-65.
34. Park, J.H., et al., *Crystal structure of the ligand-free G-protein-coupled receptor opsin.* Nature, 2008. **454**(7201): p. 183-7.
35. Dale, H.H., *The action of certain esters and ethers of choline, and their relation to muscarine.* J. Pharmacol .EXP, 1914. **6**: p. 147–190.
36. Baldwin , J.M., *The probable arrangement of the helix in G protein coupled receptors.* The EMBO Journal, 1993. **12**(4): p. 1693 - 1703.
37. Wess, J., T.I. Bonner, and M.R. Brann, *Chimeric m2/m3 muscarinic receptors: role of carboxyl terminal receptor domains in selectivity of ligand binding and coupling to phosphoinositide hydrolysis.* Molecular Pharmacology, 1990. **38**(6): p. 872-7.
38. Ichiyama, S., et al., *The structure of the third intracellular loop of the muscarinic acetylcholine receptor M2 subtype.* FEBS Lett, 2006. **580**(1): p. 23-6.
39. Wess, J., et al., *Structural basis of receptor/G protein coupling selectivity studied with muscarinic receptors as model systems.* Life Sci, 1997. **60**(13-14): p. 1007-14.

40. Caulfield, M.P. and N.J. Birdsall, *International Union of Pharmacology. XVII. Classification of muscarinic acetylcholine receptors.* Pharmacol Rev, 1998. **50**(2): p. 279-90.
41. Kurtenbach, E., et al., *Muscarinic acetylcholine receptors. Peptide sequencing identifies residues involved in antagonist binding and disulfide bond formation.* Journal of Biological Chemistry, 1990. **265**(23): p. 13702-8.
42. Lu, Z.L., et al., *The role of the aspartate-arginine-tyrosine triad in the m1 muscarinic receptor: mutations of aspartate 122 and tyrosine 124 decrease receptor expression but do not abolish signaling.* Molecular Pharmacology, 1997. **51**(2): p. 234-41.
43. May, L.T., et al., *Allosteric modulation of G protein-coupled receptors.* Annu Rev Pharmacol Toxicol, 2007. **47**: p. 1-51.
44. Wotta, D.R., et al., *M1, M3 and M5 muscarinic receptors stimulate mitogenactivated protein kinase.* Pharmacology, 1998. **56**(4): p. 175-86.
45. Ishii, M. and Y. Kurachi, *Muscarinic acetylcholine receptors.* Curr Pharm Des, 2006. **12**(28): p. 3573-81.
46. Gomeza, J., et al., *Pronounced pharmacologic deficits in M2 muscarinic acetylcholine receptor knockout mice.* Proc Natl Acad Sci U S A, 1999. **96**(4): p. 1692-7.
47. Stengel, P.W., et al., *M(2) and M(4) receptor knockout mice: muscarinic receptor function in cardiac and smooth muscle in vitro.* Journal of Pharmacology and Experimental Therapeutics, 2000. **292**(3): p. 877-85.
48. De Schryver, A.M. and M. Samsom, *New developments in the treatment of irritable bowel syndrome.* Scand J Gastroenterol Suppl, 2000(232): p. 38-42.
49. Ehlert, F.J., *Contractile role of M2 and M3 muscarinic receptors in gastrointestinal, airway and urinary bladder smooth muscle.* Life Sciences, 2003. **74**(2-3): p. 355-66.
50. Kay, G.G., et al., *Antimuscarinic drugs for overactive bladder and their potential effects on cognitive function in older patients.* Journal of the American Geriatrics Society, 2005. **53**(12): p. 2195-201.
51. Lee, A.M., D.B. Jacoby, and A.D. Fryer, *Selective muscarinic receptor antagonists for airway diseases.* Current Opinion in Pharmacology, 2001. **1**(3): p. 223-9.

52. Uchiyama, T. and R. Chess-Williams, *Muscarinic receptor subtypes of the bladder and gastrointestinal tract.* J Smooth Muscle Res, 2004. **40**(6): p. 237-47.
53. Wang, Z., H. Shi, and H. Wang, *Functional M3 muscarinic acetylcholine receptors in mammalian hearts.* Br J Pharmacol, 2004. **142**(3): p. 395-408.
54. Watson, S. and S. Arkinstall, *The G-protein Linked Receptor Facts Book, Academic Press. @* London, 1994: p. 7- 18.
55. Gromada, J. and T.E. Hughes, *Ringing the dinner bell for insulin: muscarinic M3 receptor activity in the control of pancreatic beta cell function.* Cell Metab, 2006. **3**(6): p. 390-2.
56. Levey, A.I., *Immunological localization of m1-m5 muscarinic acetylcholine receptors in peripheral tissues and brain.* Life Sciences, 1993. **52**(5-6): p. 441-8.
57. Matsui, M., et al., *Multiple functional defects in peripheral autonomic organs in mice lacking muscarinic acetylcholine receptor gene for the M3 subtype.* Proc Natl Acad Sci U S A, 2000. **97**(17): p. 9579-84.
58. Borroto-escuela, D.O. and L.a.G. Iarriccio, P, *Homology Modelling of the Structure of Human m3 Muscarinic Acetylcholine Receptor.*
59. Kubinyi, H., *[Molecular similarity. 2. The structural basis of drug design]*. Pharm Unserer Zeit, 1998. **27**(4): p. 158-72.
60. Kubinyi, H., *[Molecular similarity. 1. Chemical structure and biological action]*. Pharm Unserer Zeit, 1998. **27**(3): p. 92-106.
61. Bohacek, R.S. and C. McMartin, *Modern computational chemistry and drug discovery: structure generating programs.* Curr Opin Chem Biol, 1997. **1**(2): p. 157-61.
62. Bluml, K., E. Mutschler, and J. Wess, *Functional role in ligand binding and receptor activation of an asparagine residue present in the sixth transmembrane domain of all muscarinic acetylcholine receptors.* Journal of Biological Chemistry, 1994. **269**(29): p. 18870-6.
63. Strader, C.D., et al., *Conserved aspartic acid residues 79 and 113 of the betaadrenergic receptor have different roles in receptor function.* Journal of Biological Chemistry, 1988. **263**(21): p. 10267-71.

64. Strader, C.D., et al., *Identification of two serine residues involved in agonist activation of the beta-adrenergic receptor.* Journal of Biological Chemistry, 1989. **264**(23): p. 13572-8.
65. Strader, C.D., et al., *Allele-specific activation of genetically engineered receptors.* Journal of Biological Chemistry, 1991. **266**(1): p. 5-8.
66. Wess, J., D. Gdula, and M.R. Brann, *Site-directed mutagenesis of the m3 muscarinic receptor: identification of a series of threonine and tyrosine residues involved in agonist but not antagonist binding.* Embo Journal, 1991. **10**(12): p. 3729-34.
67. Ostopovici , L., et al., *Exploring the Binding Site of the Human Muscarinic M3 Receptor: Homology Modeling and Docking Study.* International Journal of Quantum Chemistry, 2007. **107**(8): p. 1794–1802.
68. Avlani, V.A., et al., *Critical role for the second extracellular loop in the binding of both orthosteric and allosteric G protein-coupled receptor ligands.* Journal of Biological Chemistry, 2007. **282**(35): p. 25677-86.
69. Schwartz, T.W. and B. Holst, *Allosteric enhancers, allosteric agonists and agoallosteric modulators: where do they bind and how do they act?* Trends Pharmacol Sci, 2007. **28**(8): p. 366-73.
70. Ivetac, A. and J.A. McCammon, *Mapping the druggable allosteric space of Gprotein coupled receptors: a fragment-based molecular dynamics approach.* Chem Biol Drug Des, 2010. **76**(3): p. 201-17.
71. Casarosa, P., et al., *Preclinical evaluation of long-acting muscarinic antagonists: comparison of tiotropium and investigational drugs.* Journal of Pharmacology and Experimental Therapeutics, 2009. **330**(2): p. 660-8.
72. Kato, M., K. Komamura, and M. Kitakaze, *Tiotropium, a novel muscarinic M3 receptor antagonist, improved symptoms of chronic obstructive pulmonary disease complicated by chronic heart failure.* Circulation Journal, 2006. **70**(12): p. 1658-60.
73. *Spiriva Handihaler.* The American Society of Health-System Pharmacists, 3 April 2011.
74. Fryer, A.D., et al., *Effects of inflammatory cells on neuronal M2 muscarinic receptor function in the lung.* Life Sciences, 1999. **64**(6-7): p. 449-55.

75. Jin, J., et al., *Discovery of biphenyl piperazines as novel and long acting muscarinic acetylcholine receptor antagonists.* Journal of Medicinal Chemistry, 2008. **51**(19): p. 5915-8.
76. Goodwin, J.A., et al., *Roof and floor of the muscarinic binding pocket: variations in the binding modes of orthosteric ligands.* Molecular Pharmacology, 2007. **72**(6): p. 1484-96.
77. Darden, T.A., L. Bartolotti, and L.G. Pedersen, *Selected new developments in computational chemistry.* Environ Health Perspect, 1996. **104 Suppl 1**: p. 69-74.
78. Anders, M.W., H. Yin, and J.P. Jones, *Application of computational chemistry in the study of biologically reactive intermediates.* Adv Exp Med Biol, 1996. **387**: p. 347-53.
79. Kubinyi, H., *Structure-based design of enzyme inhibitors and receptor ligands.* Curr Opin Drug Discov Devel, 1998. **1**(1): p. 4-15.
80. Kubinyi, H., *Combinatorial and computational approaches in structure-based drug design.* Curr Opin Drug Discov Devel, 1998. **1**(1): p. 16-27.
81. Wolber, G., et al., *Molecule-pharmacophore superpositioning and pattern matching in computational drug design.* Drug Discov Today, 2008. **13**(1-2): p. 23-9.
82. He, Y.X., et al., *Crystal structure and computational analyses provide insights into the catalytic mechanism of 2,4-diacetylphloroglucinol hydrolase PhlG from Pseudomonas fluorescens.* Journal of Biological Chemistry, 2010. **285**(7): p. 4603-11.
83. Kondrashov, D.A., et al., *Protein structural variation in computational models and crystallographic data.* Structure, 2007. **15**(2): p. 169-77.
84. Awale, M., et al., *Homology modeling and atomic level binding study of Leishmania MAPK with inhibitors.* Journal of Molecular Modeling, 2010. **16**(3): p. 475-88.
85. Evers, A. and T. Klabunde, *Structure-based drug discovery using GPCR homology modeling: successful virtual screening for antagonists of the alpha1A adrenergic receptor.* Journal of Medicinal Chemistry, 2005. **48**(4): p. 1088-97.
86. Wang, Y.T., et al., *Homology modeling, docking, and molecular dynamics reveal HR1039 as a potent inhibitor of 2009 A(H1N1) influenza neuraminidase.* Biophys Chem, 2010. **147**(1-2): p. 74-80.

87. Gudermann, T., B. Nurnberg, and G. Schultz, *Receptors and G proteins as primary components of transmembrane signal transduction. Part 1. G-proteincoupled receptors: structure and function.* J Mol Med (Berl), 1995. **73**(2): p. 51-
63.
88. Worth, C.L., G. Kleinau, and G. Krause, *Comparative sequence and structural analyses of G-protein-coupled receptor crystal structures and implications for molecular models.* Plos One, 2009. **4**(9): p. e7011.
89. Simms, J., et al., *Homology modeling of GPCRs.* Methods Mol Biol, 2009. **552**: p. 97-113.
90. Sousa, S.F., P.A. Fernandes, and M.J. Ramos, *Protein-ligand docking: current status and future challenges.* Proteins, 2006. **65**(1): p. 15-26.
91. Bissantz, C., G. Folkers, and D. Rognan, *Protein-based virtual screening of chemical databases. 1. Evaluation of different docking/scoring combinations.* Journal of Medicinal Chemistry, 2000. **43**(25): p. 4759-67.
92. Cole, J.C., et al., *Comparing protein-ligand docking programs is difficult.* Proteins, 2005. **60**(3): p. 325-32.
93. Taylor, R.D., P.J. Jewsbury, and J.W. Essex, *A review of protein-small molecule docking methods.* J Comput Aided Mol Des, 2002. **16**(3): p. 151-66.
94. Goodsell, D.S., *Computational docking of biomolecular complexes with AutoDock.* Cold Spring Harb Protoc, 2009. **2009**(5): p. pdb prot5200.
95. Jones, G., P. Willett, and R.C. Glen, *Molecular recognition of receptor sites using a genetic algorithm with a description of desolvation.* J Mol Biol, 1995. **245**(1): p. 43-53.
96. Jones, G., et al., *Development and validation of a genetic algorithm for flexible docking.* J Mol Biol, 1997. **267**(3): p. 727-48.
97. Verdonk, M.L., et al., *Modeling water molecules in protein-ligand docking using GOLD.* Journal of Medicinal Chemistry, 2005. **48**(20): p. 6504-15.
98. Verdonk, M.L., et al., *Improved protein-ligand docking using GOLD.* Proteins, 2003. **52**(4): p. 609-23.
99. Kini , J., et al., *Automation of process of devising newer Chromone derivatives from existing Natural and Synthetic Chromones by their Study of Structure Activity Relationship – a novel approach* Inernational Journal of Science Research 2013. **01**(04).

100. Mukhopadhyay, P.M., L . and P. Tieleman *Molecular Dynamics Simulation of a palmitoyl-oleyl phosphatidylserine bilayer with Na couterions and NaCl.* Biophysical Journal., 2004. **86**(1601-1609).
101. Wereszczynski, J. and J.A. McCammon, *Statistical mechanics and molecular dynamics in evaluating thermodynamic properties of biomolecular recognition.* Q Rev Biophys, 2012. **45**(1): p. 1-25.
102. Cornell, W.D., et al., *A second generation force field for the simulation of proteins, nucleic acids, and organic molecules.* Journal of the American Chemical Society., 1995. **117**(19): p. 5179-5197.
103. Brooks .C and C. .DA, *Simulations of peptide conformational dynamics and thermodynamics.* Chemical Reviews. , 1993. **93**(7): p. 2487-2502.
104. Levitt M, Hirshberg M, and S.R.a.D. V, *Potential energy function and parameters for simulations of the molecular dynamics of proteins and nucleic acids in solution.* Computer Physics Communications. , 1995. **91**(1-3): p. 215231.
105. Pearlman , D., et al., *Amber, a Package of Computer-Programs for Applying Molecular Mechanics, Normal-Mode Analysis, Molecular-Dynamics and FreeEnergy Calculations to Simulate the Structural and Energetic Properties of Molecules.* Computer Physics Communications. , 1995. **91** (1-3): p. 1-41.
106. Jorgensen , W., D. Maxwell , and J. Tirado-Rives, *Development and Testing of the OPLS All-Atom Force Field on Conformational Energetics and Properties of Organic Liquids.* Journal of the American Chemical Society, 1996. **118**: p. 11225-11236.
107. Cordomi, A. and J.J. Perez, *Molecular dynamics simulations of rhodopsin in different one-component lipid bilayers.* Journal of Physical Chemistry B, 2007. **111**(25): p. 7052-63.
108. Jorgensen, W.L., et al., *Comparison of Simple Potential Functions for Simulating Liquid Water.* Journal of Chemical Physics, 1983. **79**(2): p. 926-935.
109. Allen , M. and D. Tildesley *Computer simulations of liquids.* Oxford University Press, Oxford, New York., 1987.
110. Berendsen, H.J.C., D. Vanderspoel, and R. Vandrunen, *Gromacs - a MessagePassing Parallel Molecular-Dynamics Implementation.* Computer Physics Communications, 1995. **91**(1-3): p. 43-56.

111. Lindahl, E., B. Hess, and D. van der Spoel, *GROMACS 3.0: a package for molecular simulation and trajectory analysis.* Journal of Molecular Modeling, 2001. **7**(8): p. 306-317.
112. Haga, K., et al., *Structure of the human M2 muscarinic acetylcholine receptor bound to an antagonist.* Nature, 2012. **482**(7386): p. 547-51.
113. Kruse, A.C., et al., *Structure and dynamics of the M3 muscarinic acetylcholine receptor.* Nature, 2012. **482**(7386): p. 552-6.
114. Martinez-Archundia, M., et al., *Molecular modeling of the M3 acetylcholine muscarinic receptor and its binding site.* J Biomed Biotechnol, 2012. **2012**: p. 789741.
115. McGuffin, L.J., K. Bryson, and D.T. Jones, *The PSIPRED protein structure prediction server.* Bioinformatics, 2000. **16**(4): p. 404-5.
116. Burstein, E.S., T.A. Spalding, and M.R. Brann, *The second intracellular loop of the m5 muscarinic receptor is the switch which enables G-protein coupling.* Journal of Biological Chemistry, 1998. **273**(38): p. 24322-7.
117. Lin, S.S., U. Gether, and B.K. Kobilka, *Ligand stabilization of the beta(2) adrenergic receptor: Effect of DTT on receptor conformation monitored by circular dichroism and fluorescence spectroscopy.* Biochemistry, 1996. **35**(46): p. 14445-14451.